Using CFD for Blast Wave Predictions

Olav R. Hansen*, Peter Hinze, Derek Engel and Scott Davis
GexCon US, 7735 Old Georgetown Rd suite 1010, Bethesda, MD 20814
***Email: olav@gexcon.com**

Abstract

Explosions will, in most cases, generate blast waves. While simple models (*e.g.*, Multi Energy Method) are useful for simple explosion geometries, most practical explosions are far from trivial and require detailed analyses. For a reliable estimate of the blast from a gas explosion it is necessary to know the explosion strength. The source explosion may not be symmetric; the pressure waves will be reflected or deflected when hitting objects, or even worse, the blast waves may propagate inside buildings or tunnels with a very low rate of decay. The use of computational fluid dynamics (CFD) explosion models for near and far field blast wave predictions has many advantages. These include more precise estimates of the energy and resulting pressure of the blast wave, as well as the ability to evaluate non-symmetrical effects caused by realistic geometries, gas cloud variations and ignition locations. This is essential when evaluating the likelihood of a given leak source as cause of an explosion or equally when evaluating the potential risk associated with a given leak source for a consequence analysis.

In addition, unlike simple methods, CFD explosion models can also evaluate detailed dynamic effects in the near and far field, which include time dependent pressure loads as well as reflection and focusing of the blast waves. This is particularly valuable when assessing actual near-field blast damage during an explosion investigation or potential near-field damage during a risk analysis for a facility. One main challenge in applying CFD, however, is that these models require more information about the actual facility, including geometry details and process information. Collecting the necessary geometry and process data may be quite time consuming. This paper will show some blast prediction validation examples for the CFD model FLACS. It will also provide examples of how directional effects or interaction with objects can significantly influence the dynamics of the blast wave. Finally, the challenge of obtaining useful predictions with insufficient details regarding the geometry will also be addressed.

Background

Recent accidents like Texas City (CSB, 2007), Buncefield (Buncefield Investigation Report) and Danvers (CSB Investigation Report, 2007) remind us of the potential for blast waves from vapor cloud explosions, confined or unconfined, to cause severe damage to plant and surrounding buildings. One of the most widely used methods for evaluating the blast potential from vapor cloud explosions, the TNO Multi-Energy method (van den Berg, 1985), can to some extent be classified as a back-of-the-envelope tool and has not changed much since it was developed 20 years ago. The available combustion energy from a potential vapor cloud inside the plant together with an anticipated explosion strength are used to create blast-curves. The Multi-Energy method is illustrated in Figure 1. Similar methods like Baker-Strehlow (Baker *et al.*, 1983) and

CAM (Puttock, 1995) also incorporate findings from experiments to make correlations for source strength.

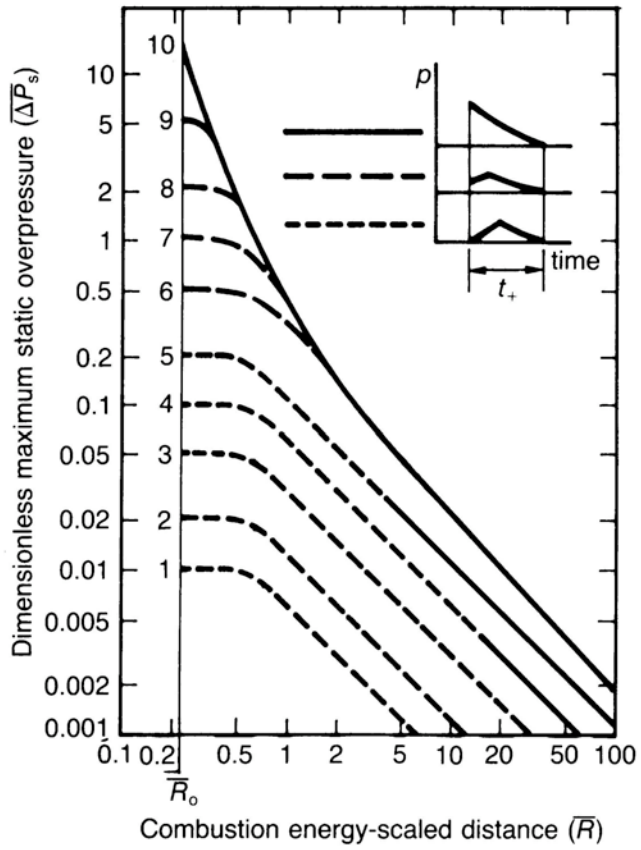

$$\overline{\Delta P_s} = \frac{P_{static} - P_o}{P_o}$$

P_o = ambient pressure

P_{static} = static total blast pressure

$$\overline{R} = R[P_o / E]^{1/3}$$

R = distance from the center of explosion

E = total available combustion energy

Figure 1: Illustration of TNO Multi-Energy method (van den Berg, 1985). A scaled distance is estimated based on the available combustion energy of a gas cloud inside a plant. With this scaled distance, and assumption of explosion strength (curves 1 to 10 representing 10 mbarg to ~10 barg source strength), the pressure as a function of distance (see above plot) and other parameters can be estimated. This method has been used to predict the quantity of fuel involved and the consequences of vapor cloud explosions

Some weaknesses with these methods are:

- These methods have limited ability, if any, to predict the actual explosion source strength or dynamics. Source explosion strength has to be estimated based on limited experimental data, predictions using more detailed CFD tools, or estimated near-field blast damage.
- Some of the methods are calibrated based on experiments at limited scale, and are incapable or inappropriate for scaled-up explosions
- These methods have limited ability to take into consideration directional effects, asymmetric explosions, or effects due to partial confinement
- Blast-wave interaction with structures in near- and far-field, or the effect of protection walls cannot be predicted

Alternately, Computational Fluid Dynamics (CFD) models are capable of modeling the abovementioned effects, but may face other challenges. In order for a model to be used as a predictive tool, its validity and capability to predict explosion phenomena must be demonstrated. One particular challenge is to properly resolve and represent shock waves. A shock wave is considered a discontinuity, where the leading edge of a pressure curve rises abruptly. Unless some shock-conservation method is applied, such a sharp front will become smeared using a CFD-tool. In addition to predicting a slower pressure rise, this may also lead to an under-prediction of the maximum overpressure.

One main purpose of this paper is present validation data for the CFD-software FLACS against a wide-variety of explosion field experiments, ranging from (1) symmetric, unconfined geometries to (2) asymmetric, partially confined and congested modules, to (3) total confinement. From previous studies (*e.g.*, van Wingerden *et al*., 1995), FLACS is expected to yield reasonably accurate predictions for explosion source strengths, asymmetric effects, blast wave propagation at the various scales and complexities of the experiments. Another purpose of this paper is to present far-field blast validation data for FLACS. The characteristics of the experiments to be modeled vary significantly and are listed below. All of the validations were performed against experiments using mixtures of methane, or methane dominated natural gas, and air:

- 6 MERGE geometries 46m^3 and 365m^3 unconfined explosions (Mercx *et al.*, 1994)
- 4 BFETS Phase II 1600m^3 tests, semi-confined, low/high congestion density, center and end ignition (SCI, 1996, Selby and Burgan, 1998)
- 4 BFETS Phase II 1600m^3 tests with water deluge, high congestion density, center and end ignition (Selby and Burgan, 1998)
- 4 HSE-Phase 3A 2600m^3 tests with low confinement and different ignition locations (Al-Hassan and Johnson, 1998)
- 6 Phase 3B 2600m^3 module tests, 6 different gas cloud sizes from 10% to 100% filled (Johnson *et al.*, 2002)
- 6 tunnel test 150 and 220 m^3, different tunnel designs (Zipf *et al.*, 2007)

Compared to simple blast prediction models that will immediately provide an answer, more effort and time are required when using CFD to accurately describe the details of the experiment. While simulation times may be on the order of hours to days, what tends to be more critical is the necessity for detailed modeling of the geometry if accurate pressure predictions are to be expected. Manually constructing a detailed model, say for an onshore facility, may require man-years of effort. An alternative, such as laser scanning, is still a fairly expensive option and may only be worthwhile if the constructed geometry model can also be used for other purposes than the blast study. If a CAD model of the facility does exist, this can usually be imported into the CFD-model and utilized. If the model is in the early design stages or incomplete, the density of pipe arrays may need to be increased to a more realistic level (anticipated congestion) in order to predict the explosion development correctly. Such anticipated congestion methods (ACM, see Hoorelbeke *et al.,* 2006) are widely used in blast studies, and involve much less work than the construction of the complete geometry. However, in order to perform more efficient siting studies using CFD for existing facilities, for which no CAD model exists, there may be a need for a quick screening approach. In the second part of this paper such a method is described, in which the main geometry structures (main confinement, walls and decks) are modeled in some

detail, whereas the remainder of the piping and structures are represented by regular obstruction arrays that are representative of the actual equipment density. In this way it will be possible to benefit from many of the advantages of CFD, but at the same time bypass the very time-consuming geometry modeling process for the initial screening calculations

FLACS CFD Model

The development of the FLACS CFD software started in 1982 (Hjertager, 1995). The initial ambitions were to predict the consequences of gas explosions on oil and gas offshore installations (Bakke and Hansen, 2003). The functionality has gradually been extended to include the prediction of gas dispersion of flammable and toxic gases (Hanna *et al*., 2009), as well as far-field blast waves (van Wingerden *et al.*, 1999) and recently liquid releases with pool spill and spread models (Hansen *et al.,* 2007) Models to predict the release of flashing jets are under development (Ichard *et al.*, 2009). While the modeling of natural gas and hydrocarbon explosions have been the main focus, a considerable effort has also been invested in the accurate modeling of hydrogen dispersion and explosion effects (Middha and Hansen, 2009).

In 1994 developments were incorporated that improved the ability to model far field pressures with FLACS. Firstly, a multiblock concept was developed, so that it was possible to calculate the explosion using the full Navier-Stokes equations in the primary domain, and outside this domain, a number of domains could be added for which an Euler FCT-solver could be applied. Furthermore, new non-reflecting boundary conditions had been developed (PLANE_WAVE boundary condition in FLACS), which would detect a pressure wave approaching the boundaries and ensure that the pressure wave would leave the domain, or propagate along a boundary, without returning unphysical reflections. When initially released, a small validation study was performed, which demonstrated reasonable results for a handful of explosion scenarios (van Wingerden *et al*., 1995).

One major problem with the multiblock concept was that the coupling between different domains was very sensitive regarding stability, and much shorter time steps were needed than was recommended to obtain reliable explosion results with FLACS. When reducing the time-steps to the required level, this would frequently change the pressure predictions with FLACS. As a consequence it became very challenging to reliably predict far-field blast waves. Further limitations with the multiblock system were that the blast blocks could only handle zero and one porosities, and could not handle pressure relief panels.

In 2005 GexCon therefore stopped recommending the use of the multiblock concept for pressure waves in the far field, and now one single block in the calculations was recommended.

FLACS Guidelines and Modeling Approach

The FLACS software is widely used for safety studies and risk assessments on petrochemical installations and elsewhere. Important safety decisions are made based on the output from FLACS, and for that reason it is very important that results are reliable. Application oriented validation has therefore been of high importance when developing FLACS.

The primary application area for the explosion models in FLACS has been oil and gas platforms as well as safety considerations for offshore petrochemical structures. For these situations blast loading on the module walls where the explosion takes place has been of primary importance, whereas the far-field blast pressures have been less critical. With increasing use of CFD software for onshore safety studies, the far-field pressure propagation and siting issues will be of importance.

With the previously used multi-block approach, it could sometimes be complicated to perform a blast study. Due to the previously mentioned need for very short time steps, situations frequently were seen where the source strength predictions became too high or too low as a result of the need for a finer time step. With the new approach this problem has disappeared, and the studies are more straightforward to perform. There is, however, a requirement for a short time step during the blast propagation simulation in order to resolve the pressure waves. In order to keep the recommended time step setting for explosion simulations, but at the same time maintain good resolution during the far-field blast propagation, a new switch has been introduced in FLACS. With the new option

STEP = "KEEP_LOW"

the time step will be reduced the normal way when the explosion develops and gets stronger. But after the maximum pressure when normal explosion calculations decrease in strength, this option ensures that the shortest time step determined during the explosion is also used for the rest of the pressure wave propagation process.

It is also required to apply "PLANE_WAVE" non-reflecting boundary condition. Except for these additional recommendations, all scenario guidelines will be the same as applied in normal explosion studies.

Guidelines are issued based on validation tests for most applications. Regarding far-field pressures, very limited validation simulations have been performed after 1994, so the guidelines in general follow guidelines needed for gas explosions, with the addition of the switch as well as using the non-reflecting boundary condition previously mentioned above.

When it comes to grid embedding, the main guidelines are developed to ensure accurate predictions of the source strength. The following guidelines were applied in these simulations:

- The domain must be defined to include the explosion as well as all targets. It is also recommended that the grid extends a certain direction outside the gas cloud in any open direction.
- Cubical cells must be defined inside gas cloud and vicinity. Maintain the grid spacing all the way to the boundary in the direction of the external blast targets.
- The maximum acceptable grid size in each direction will be to resolve the gas cloud (or congested region, whichever is smaller) by
    - ~8 cells if cloud is confined on both sides
    - ~10 cells if cloud is confined on one side (*e.g.*, ground)
    - ~13 cells if the cloud is unconfined

Max $\Delta X, \Delta Y, \Delta Z = 0.1 \times \text{CloudVolume}^{1/3}$ has also been used as a criterion

- The grid size may be gradually increased towards the boundary in directions other than those towards the external blast targets. Maximum stretch factor from one cell to the next ~1.2
- Main confining walls should be on grid lines
- It is recommended to repeat simulations, at least for the source region, with more than one grid resolution; this is to ensure that the grid dependency is not too high. If variability is seen (in particular for regularly repeated obstructions this may be seen) it is recommended to select among the finer grids giving source pressures in the higher range observed.

Experimental Uncertainty and Measurement Aspects

When performing a validation study, the model performance will not only depend on the quality of simulations but also the quality of the experimental recorded measurements. As the experiments presented in the present study were performed by some of the most experienced test organizations in the world, it is reasonable to believe that the results for explosion pressures in the source region are of decent quality. It is GexCon's understanding that only a couple of the experiments presented herein were repeated (*e.g.*, BFETS Phase 2, scenario 1 and 2). During the BFETS Phase 2 tests, a variability of less than 10-20% was observed for maximum pressures, however an even larger variation was observed for certain local sensors. The HSE Phase 3A tests were not repeated, but some later experiments in the same test series were repeated, with a large variation in maximum source pressures (up to factor of two for low pressure levels and factor of ten for the higher pressure levels). For the other tests employed in this study, an evaluation of similar tests (*e.g.*, MERGE tests with other gases) using different fuels can sometimes be used to judge the quality of test results; however, for the presented data it can in general be difficult to evaluate whether a repeated test can be expected to be within ~10% or a factor of two of the pressure level.

Conversely, we would expect more significant experimental variability for external blast sensors. In most of the tests presented, so-called skimmer plates were used to measure the side-on blast, *i.e.*, the plates are mounted vertically with respect to a given direction so that the pressure waves are expected to arrive parallel to the plates. In theory, this setup avoids reflective contributions (from normal or head-on contributions) on the sensors. One main challenge for designing explosion experiments is that one cannot always predict which direction the pressure waves will propagate. In fact, in many cases pressure waves from different directions may arrive at a given sensor at different times. This problem will be most significant in the near field, where many of the explosion tests do not report pressures from some of the nearer external sensors, likely due to abnormalities of this kind. Figure 2 shows an illustration of this phenomenon (blast waves arriving from various directions non-parallel to sensors), as well as some examples of blast pressure observations from experiments.

For some of the experimental data, an extremely thin pressure peak is observed and is possibly due to some kind of reflections of pressure waves inside the sensor. When performing model evaluations these extremely thin pressure peaks should likely be ignored and the data filtered. This type of filtering was employed in some test series, *e.g.*, BFETS Phase II, HSE Phase 3A and

Phase 3B, where transient pressure durations of 1ms or shorter were removed (early BFETS tests) or the time-dependent pressure curves were smoothed before extracting the maximum pressures (1.5 ms running average was used for HSE Phase 3A and Phase 3B). This methodology will to some extent remove and correct for these anomalously high peaks. However, such an averaging and filtering process was not performed on the pressure traces for the MERGE experiments.

In conclusion, significant uncertainty may exist in the experimental observations due to both the variability that can exist in explosion experiments and complications in measurements for the external sensors. Therefore, caution in interpreting the data is justified when performing model evaluations.

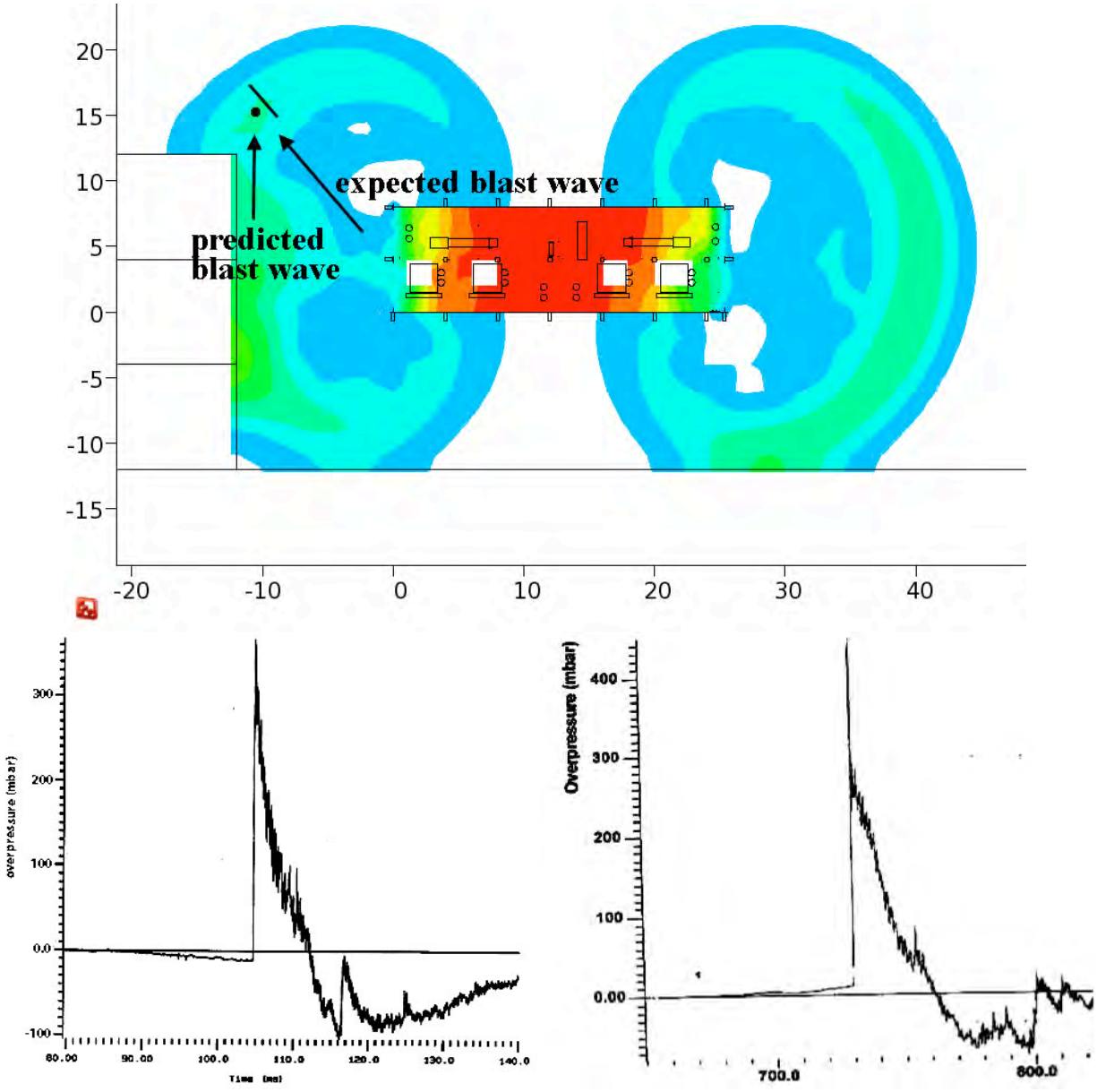

Figure 2: Illustration; sensor orientation versus blast direction (upper picture), examples of far-field blast recordings (lower picture). Lower left image - MERGE blast curve: 360 mbar is reported as the maximum pressure from the pressure trace despite very minor impulse above 300 mbar. Lower right image – HSE Phase 3A: similar example where the maximum recorded pressure is ~450 mbar (very minor impulse above 250 mbar) yet the reported pressure was 291 mbar after filtering the data using a 1.5 ms averaging algorithm.

Validation Study Against Experiments

The following will present all of the validation studies considered for the present work. The TNO Multi-Energy method predictions will also be compared against each experimental study. When using the TNO-method, we have estimated the available energy using the volume of stoichiometric gas in the "congested" region and the heat of reaction for stoichiometric methane-(or natural gas) air mixtures of 3.22 MJ/m^3. Along with FLACS predictions, representative curves using the TNO Multi-Energy method will also be presented.

MERGE

The MERGE experiments (Mercx *et al*., 1994) were performed by British Gas (was later Advantica and now Germanischer Lloyd) at the Spadeadam test site in the UK. The tests were financially supported by the European Commission, and were part of a larger project. Among several other partners, TNO performed small-scale experiments (Mercx *et al.*, 1996 describes the continued EMERGE project) and CMR (GexCon) contributed with wind tunnel testing on turbulence generation in addition to modeling. Tests were performed in six different experimental geometries by British Gas. Four cases, A, B, C and D were at medium scale (4m x 4m x 2m obstruction array with 45m^3 flammable cloud), whereas two cases E and C* were at large scale (8m x 8m x 4m obstruction array with 360 m^3 flammable cloud). Some characteristics of these geometries can be found in Table 1, and illustrations can be found in Figure 3.

Table 1: Overview of British Gas MERGE Experiments

Test	Number of pipes	Pipe diameter	Scale
MERGE-A	20 x 20 x 10	4.3 cm	Medium (45m^3)
MERGE-B	30 x 30 x 15	4.1 cm	Medium (45m^3)
MERGE-C	10 x 10 x 5	8.6 cm	Medium (45m^3)
MERGE-D	16 x 16 x 8	8.2 cm	Medium (45m^3)
MERGE-E	10 x 10 x 5	16.8 cm	Large (360 m^3) ~2:1 scale of C
MERGE-C*	20 x 20 x 10	8.2 cm	Large (360 m^3) ~2:1 scale of A

In the experiments there was a range of pressure sensors inside the congested region. In the far field there were three external sensors in most tests. For the medium-scale tests, these sensors were located at a distance of 4m, 12m and 24m from the center, and for the large-scale tests, the sensor positions were 8m, 24m and 48m from the center. The positions of these sensors are illustrated in Figure 4.

The test geometries were modeled as accurately as possible for all simulations. Scenario parameters like cloud size, gas concentration, ignition location and measurement locations were

implemented as described in the test report. Based on guidance for simulating pressure waves propagating in the far field, the time step switch KEEP_LOW was applied as well as the non-reflecting boundary conditions. To limit computational needs, two planes of symmetry were used in the simulations, and only one quarter of the geometry was modeled.

One main challenge in setting up these calculations was the choice of grid. These type of geometries, with regularly spaced repeated obstructions, may be particularly susceptible to grid dependency in simulation results. Grid guidelines will require a minimum of 10 grid cells across the gas cloud (vertical direction), so grid sizes should be less than 20cm (medium scale) and 40cm (large scale). There is a further requirement that there should be at least one grid cell for each repeated object. For MERGE-B the grid should therefore be finer than 13.3cm.

To evaluate the possible grid dependency issues, each test was simulated with 4-5 different grids, all within the guidelines (except for MERGE-B, where only the two finest grids fulfilled the requirements). Some grid dependency was observed for the explosion pressure inside the congested region, with only two cases (both for MERGE-E) of the approximately 25 simulations having a deviation of more than +/- 30% from experiment. In most cases there was approximately 20-30% pressure variability among the different grid resolutions, with the higher values corresponding well with the experimental observations.

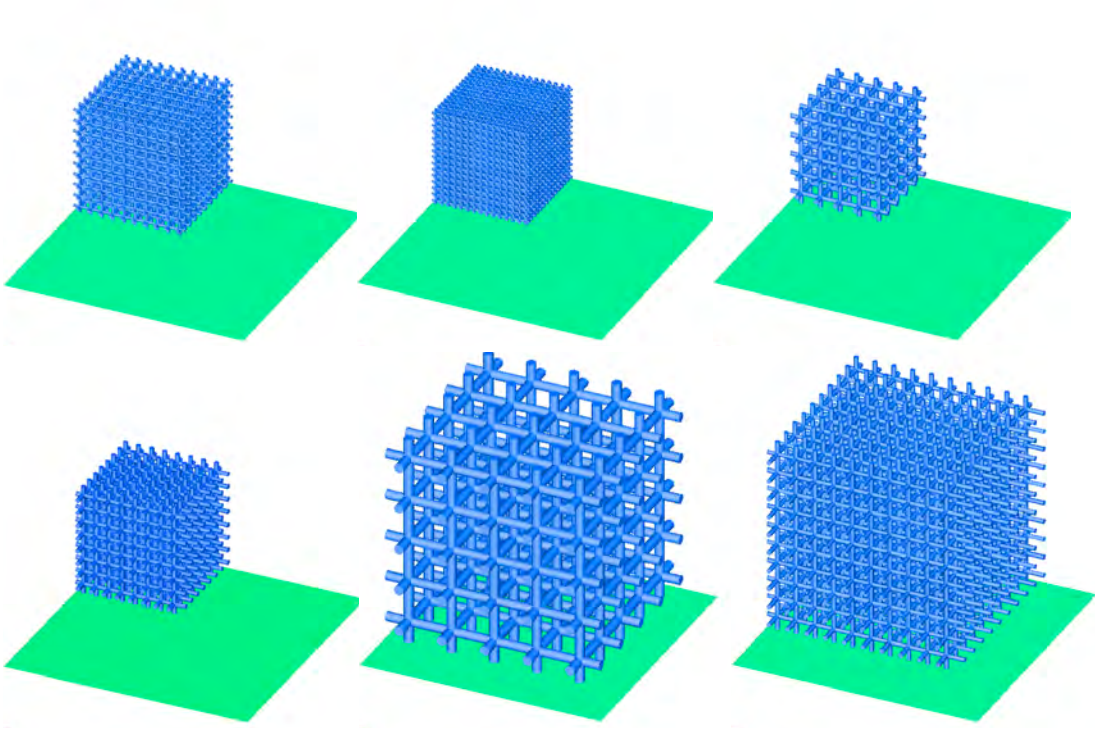

Figure 3: Illustration of MERGE geometries A (upper left), B (upper middle), C (upper right), D (lower left), E (lower middle) and C* (lower right). The obstruction arrays for geometries A-D are 4m x 4m x 2m, whereas MERGE E and C* have dimensions 8m x 8m x 4m.

In Figure 4 two examples of simulated maximum pressure contours near ground level can be seen. The upper plot shows the MERGE-C* large scale test, whereas the lower plot shows the Merge C medium-scale test.

In Figure 5, the predicted versus observed pressures are shown for the six MERGE experiments. It can be seen that FLACS predicts the explosion source pressures well for the six cases as well as the far-field pressures for weaker explosions (Merge C and E). It can also be seen that the simulations typically under predict the far-field pressures for the stronger explosions by about a factor of two. Figure 6 compares the simulated pressure curves for 4-5 different grid resolutions with one experimental example for a weak explosion (Test C, sensor at 12m) and a strong explosion (Test C* at 48m). It can be seen that the grid dependency for the far-field pressure is low for both cases. For the weak source explosion, the simulated maximum pressure resembles the experimental observations very closely, whereas the predicted pressure impulse is somewhat stronger than observed. For the strong source explosion case, it can be seen that the pressure peak is under-predicted in the far field (by about a factor of two), but that the predicted impulse (area under the pressure curve) is closer to that observed.

In addition, the simulations using the finest grid (15 cm) for Merge C* sensor 13 resulted in a predicted pressure trace that most closely resembled experimental data (highest pressure of 6 kPa and the sharpest peak). It should also be mentioned that in this simulation the source pressure was under-predicted by 20% relative to experiment, and had the predicted source pressure been closer to experiment we would likely have seen even closer far-field pressure predictions. One notable difference between experiment and simulation is the leading edge or vertical front of the pressure wave (shock-front) in the strong explosion experiments. Experimentally there is an abrupt pressure rise (or discontinuity) that tends to be smeared in the numerical simulations. We will come back to this issue in the discussion chapter.

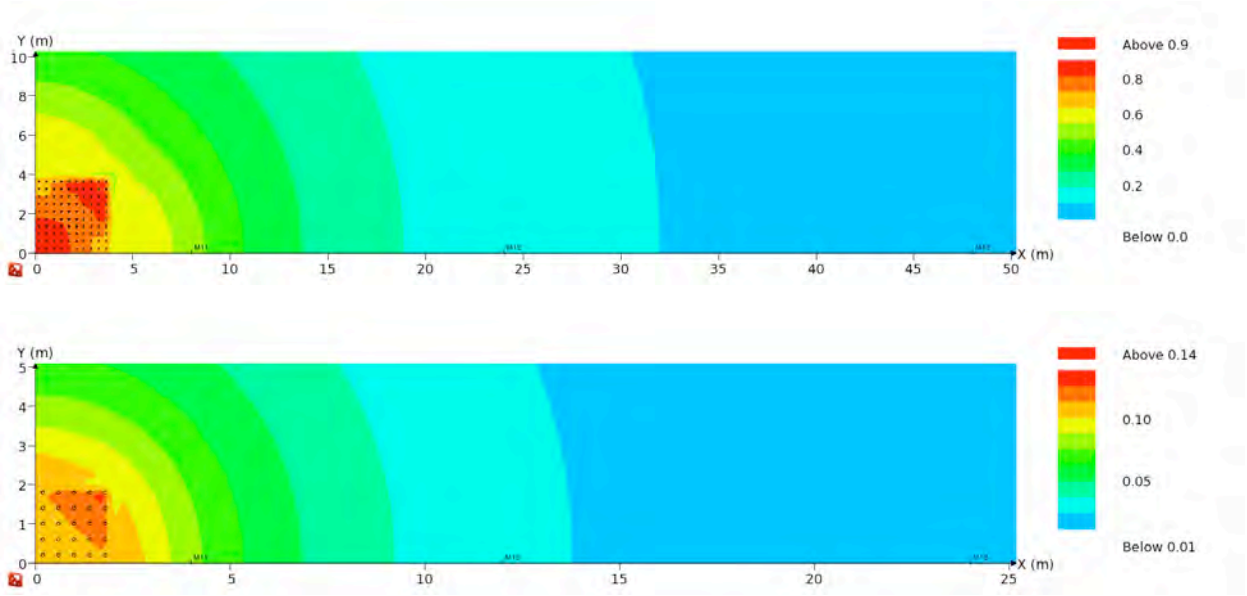

Figure 4: Simulated maximum pressure contour for large-scale test MERGE-C* (top) and medium-scale test MERGE-C (bottom)

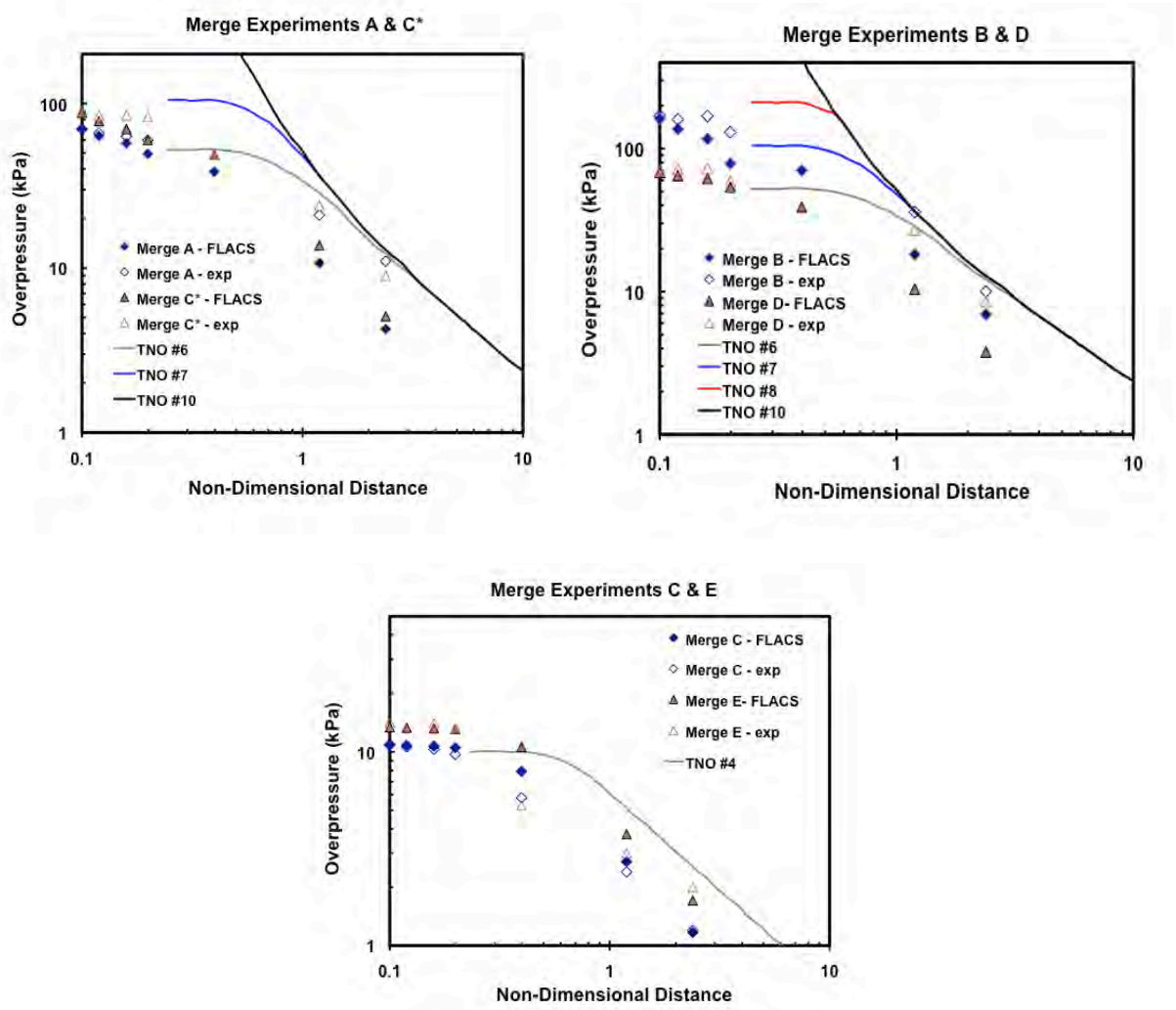

Figure 5: Pressure versus combustion-energy scaled distance for the six MERGE experiments and simulations. TNO Multi-Energy curves are shown for comparable source pressure.

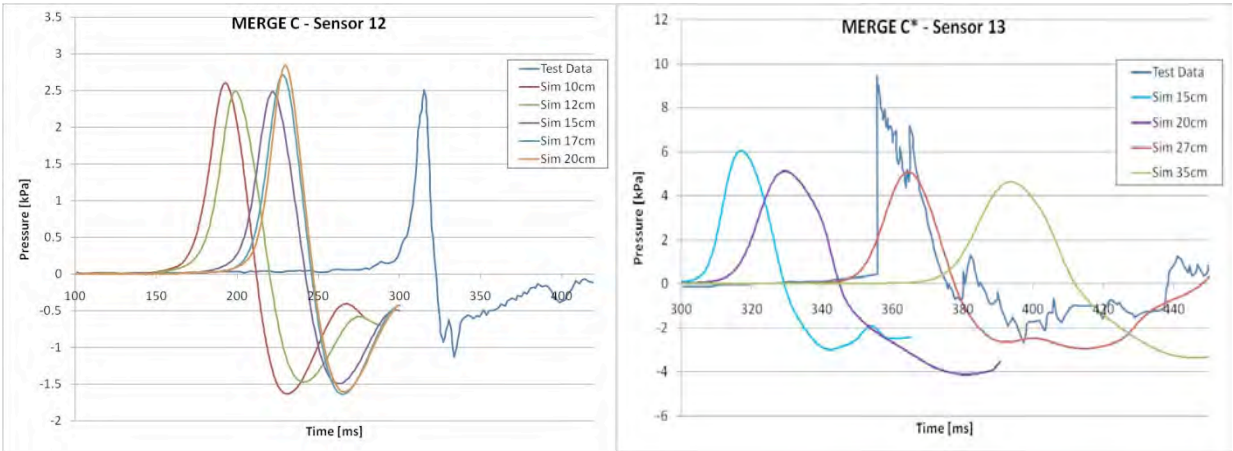

Figure 6: Example of pressure predictions MERGE C 12m (left) and MERGE C* 48m (right). Reproduced curves from experiments are shown together with the simulated pressures.

BFETS Phase II Experiments

The Blast and Fire Engineering for Topside Structures project (BFETS) was a joint industry project with the participation of a number of oil and gas companies to study explosion and fire loading to typical offshore oil and gas installations. The project was coordinated by the Steel Construction Institute (SCI). One part of the project was large-scale explosion experiments, and these were performed by British Gas (Advantica) at their Spadeadam test site from 1994 to 1997. A test program of 27 different large-scale explosion experiments was carried out. Many of the experiments were used in a blind model evaluation exercise, in which model developers were invited to predict the outcome of explosion tests in 1500m^3 natural gas and air mixture (test rig dimensions were 25.6m x 8m x 8m). The models of the BFETS test geometries used in this study are shown in Figure 7. The low congested rig (upper picture) was used for the first two scenarios (Tests 1-6), whereas the high congested rig (lower picture) was used for Tests 7-23. In this blast validation study we will simulate the first eight BFETS scenarios in which experiments where performed. These include center and end ignition cases for both low-obstacle density and high-obstacle density test geometries. To further illustrate the benefit of water deluge to limit far-field pressures, and the ability of FLACS to model this phenomenon, four experiments with water mitigation are included. These include center and end ignited scenarios in the geometry with high obstruction density, using deluge from MV57 nozzles (~17 liter/m^2/min) and from large droplet nozzles (LDN, ~27 liter/m^2/min). An overview of these experiments can be found in Table 2:

Table 2: Overview of British Gas BFETS Experiments simulated in this study (Selby, 1998)

Test	**Congestion**	**Ignition**	**Water mitigation**	**Pressures inside test rig**
BFETS 1	LOW	Center	No	~ 50 kPa
BFETS 2	LOW	End	No	< 50 kPa
BFETS 12	HIGH	Center	No	110 to 230 kPa
BFETS 7	HIGH	End	No	120 to > 440 kPa
BFETS 11	HIGH	Center	MV57	70 to 130 kPa
BFETS 9	HIGH	End	MV57	10 to 80 kPa
BFETS 10	HIGH	Center	LDN	40 to 100 kPa
BFETS 8	HIGH	End	LDN	10 to 50 kPa

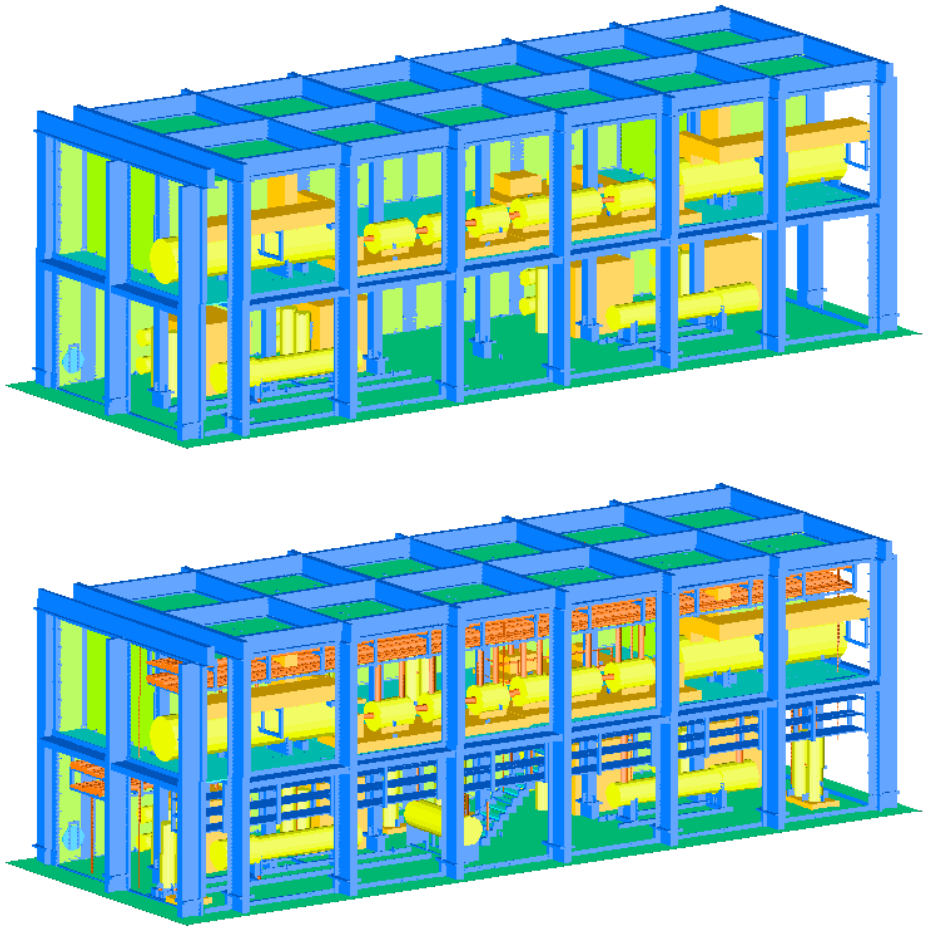

Figure 7: Illustration of BFETS geometries, the geometry with low obstruction density is shown in the upper picture and the high obstruction density in the lower picture. Front wall has been removed on the picture to visualize the inside geometry details.

The simulations were performed according to standard simulation guidelines, with the recommended modifications when modeling far-field blast pressures (STEP=”KEEP_LOW” switch and non-reflecting boundary conditions). Simulations were performed using both a 1m and 0.5m grid resolution. Comparable results were observed and the results presented in the following were obtained using a 0.5m grid.

Figure 8 provides an example of a predicted maximum pressure distribution. In this scenario the gas cloud is ignited at its edge (end of the module), and it can be seen that the resulting blast contour becomes highly non-symmetric. A 3D distribution of pressure shortly after flame exits the test rig is also shown, which again highlights the non-symmetric nature of such a test. The 11 different external sensors used for observations of external pressures can be found in the first plot (Monitors 31-41 on the plot).

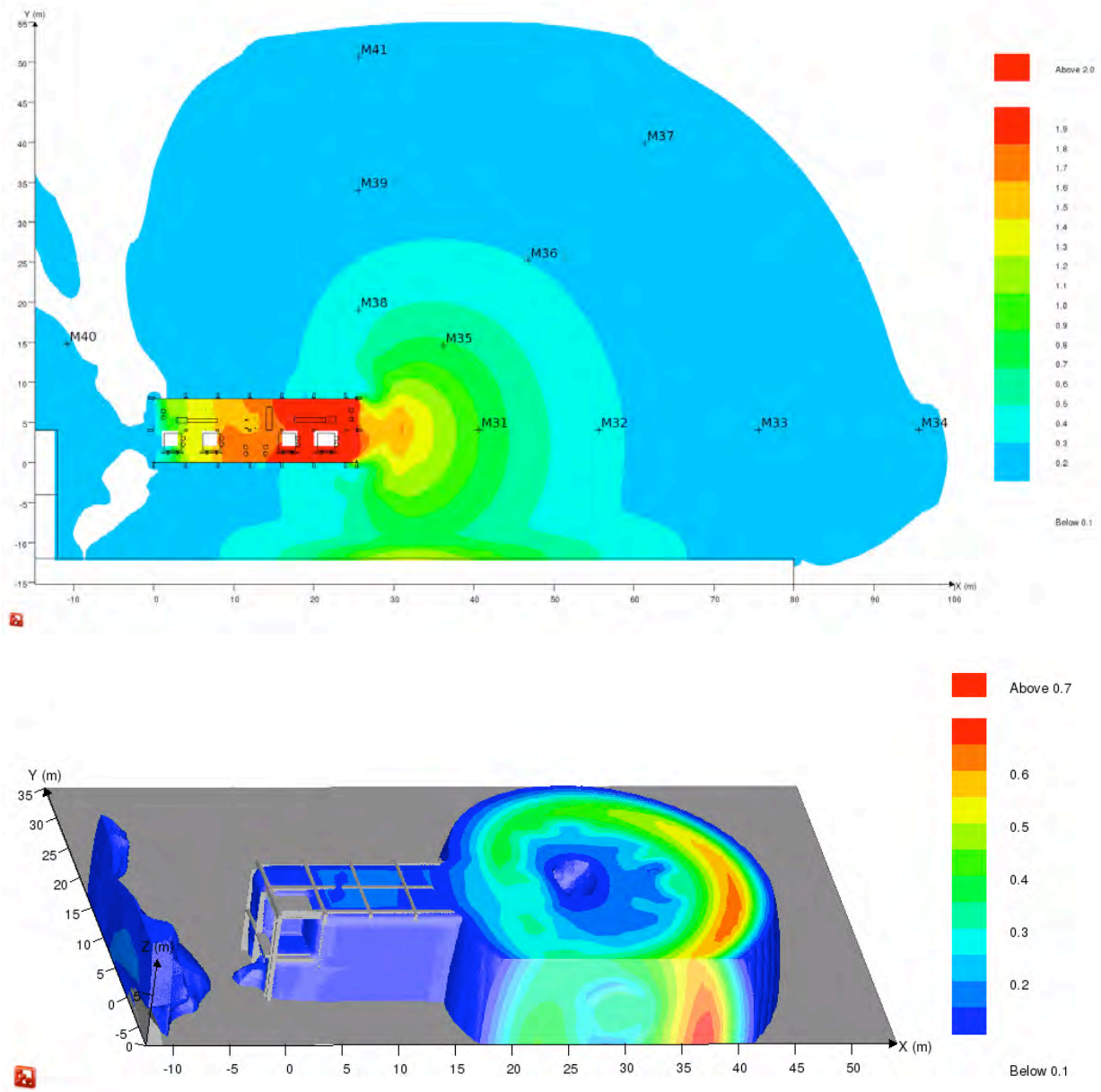

Figure 8: Simulated maximum pressures for BFETS test 7 (upper plot) and 3D pressure distribution just after the exit of the flame (lower plot). The non-symmetrical nature of such explosion scenarios is clearly illustrated.

Figure 9 shows comparisons between experimentally recorded pressures (peaks shorter than 1 ms are removed in test report) and simulated pressures for the experiments without water deluge. For all four cases, it can be seen that FLACS simulations very closely reproduce the observed asymmetric overpressures inside the test geometry. For the far-field overpressures the correlation between FLACS predictions and the experimental results is generally very good, with only a limited under-prediction in the far field for the strong cases. For the weak cases, we can observe that the overpressures (test and simulation) will follow the trends from the TNO Multi-Energy curves for associated source pressure level. However, due to geometry and asymmetric effects, there are frequently differences by more than a factor of five between TNO Multi-Energy predictions and actual observations or simulations. In addition, it appears that the experimental

data cannot be accurately predicted using only one TNO Multi-Energy curve due to the same geometric and asymmetric effects, and as such, the utility of this method can be very conservative for these types of explosions. For most cases in the high congestion density geometries, we can see that the far-field blast pressures are bound by the strong TNO Multi-Energy curve. There are however examples of points above this curve due to directional effects, as can be seen both in tests (even after 1 ms cut-off of high pressure peaks) and simulations.

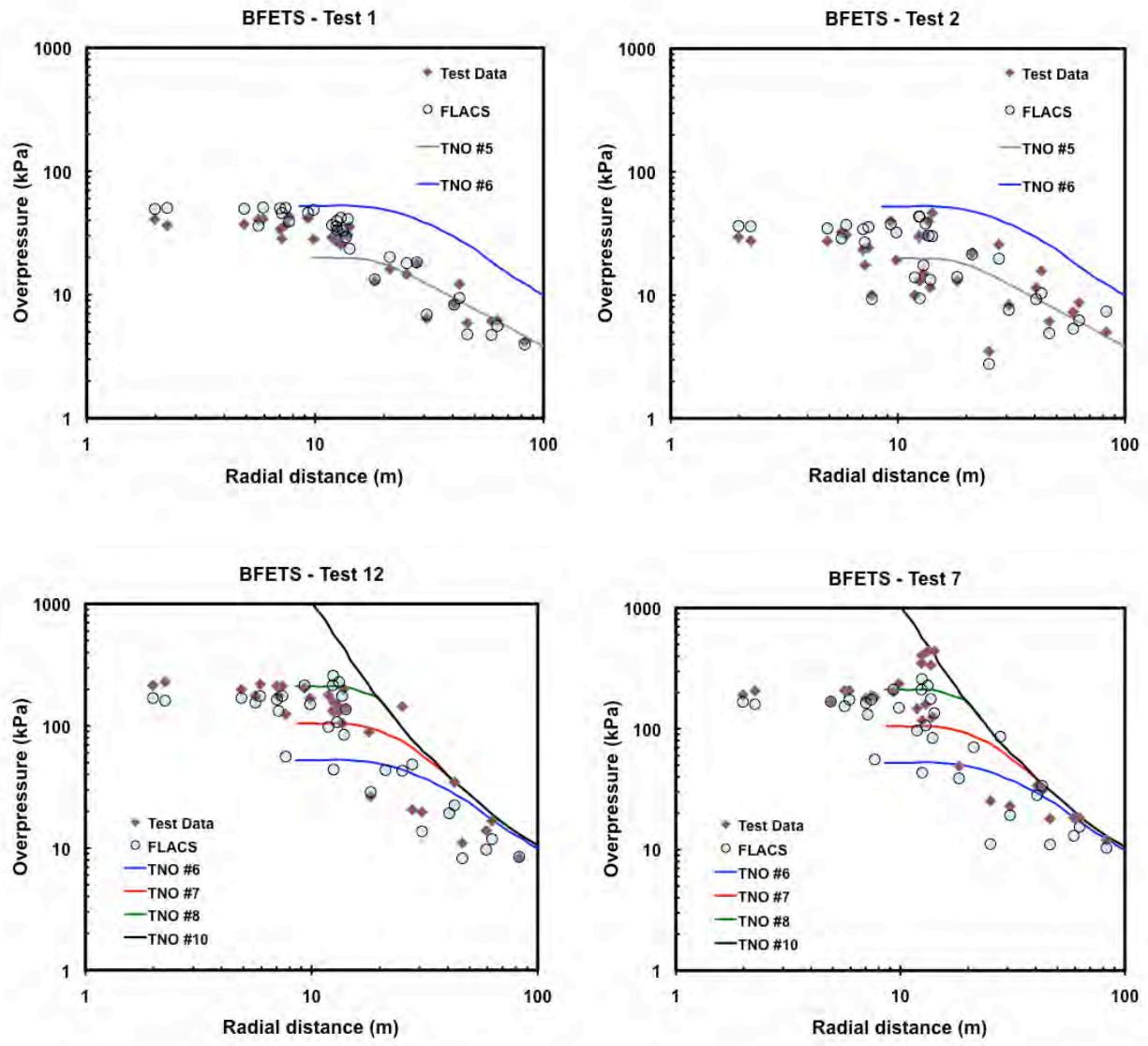

Figure 9: BFETS simulations compared to experiments, low congestion density (upper plots) versus high congestion density (lower plots), central ignition (left plots) versus end ignition (right plots).

To evaluate the slight under-prediction in the far field for the strong explosions, we have plotted the simulated pressures versus tests observations (manually digitalized from GexCon, not originals) at distances 63m (PE-2) and 83m (PE-4) from the center of explosion in Figure 10. It can be seen that there are many similarities between the simulated and observed overpressures. For the centrally ignited test, there seems to be a 2nd peak (as well as a 3rd peak) developing

about 30-40ms behind the first peak, which is not captured in the simulations. The origin of this is unclear, it could have been caused by the external explosion from the other end of the rig (which was likely made stronger by the presence of a small hill 12m away) or it could have been caused by a reflection from the parallel 4m tall hill about 12m away from the test geometry. The pressure waves from such secondary sources may oftentimes arrive from other directions, and could then be reflected on the sensor (recording a higher pressure than the actual side-on pressure). For the end ignition test (test 7) the curve is quite similar for PE-2 (except a very thin peak which is missed in the simulation). On the most remote sensor the pressure level is again comparable (except for a very thin transient), but here the impulse and pulse duration are severely overestimated. A closer look at the test results at this sensor indicates that the sensor seems to have failed after the peak has been reached, and it can be assumed that the negative slope is inaccurate. Compared to the duration of the pressure peak at 63m distance, it would be expected that the duration of the pressure peak should be at least 3 times longer than reported and closer to predictions.

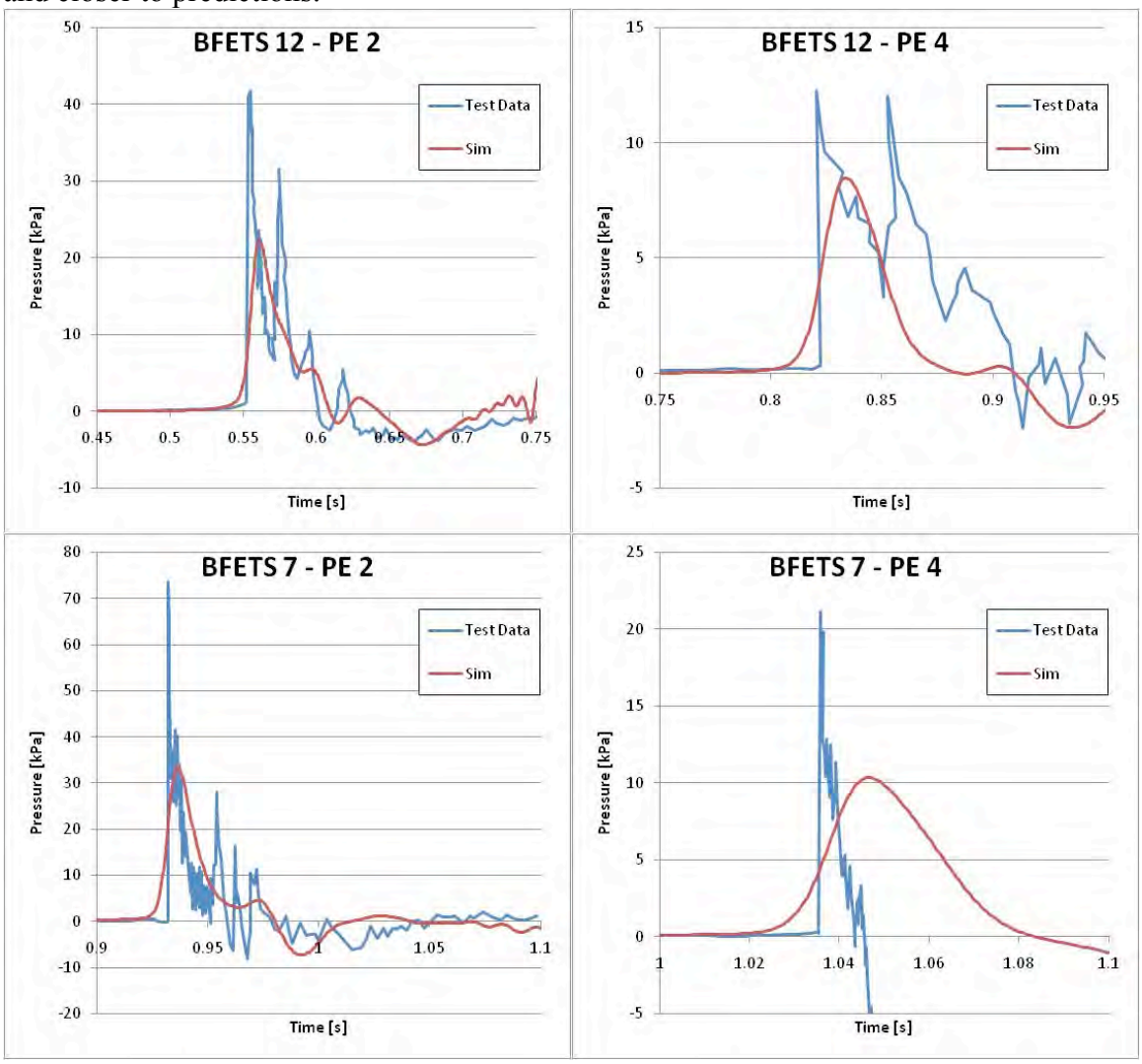

Figure 10: Examples of curve comparisons, BFETS test 12 (upper, end ignition) and test 7 (lower, center ignition) at distances 63m (left) and 83m (right) from center.

To limit the near-field and far-field blast pressures there may be different approaches of mitigation. One approach, which is used at many oil and gas offshore installations to mitigate explosion pressures, is water deluge activated at significant gas detection. During the BFETS experiments and later HSE-3A experiments the efficiency of water mitigation to limit explosion pressures, both in the near-field and far-field, was tested. Water mitigation models were included in the FLACS model in 1993, prior to the BFETS experiments being performed. Prior to this, CMR (GexCon) and British Gas had performed water deluge explosion experiments at smaller scales. Not only were the BFETS tests and later the HSE Phase 3A unique being at larger scales than previous test series, but these were also valuable as far-field blast pressures were recorded.

When applying water deluge for explosion mitigation, the sprinklers have to be activated prior to a gas cloud being ignited. After ignition, the turbulence created by the sprays will initially accelerate the flames, so that in the initial phases the pressures may increase as a result of deluge. When the deluge system is properly defined (sufficient amount of water relative to the confinement-scale-congestion), the droplets will break-up in the accelerated flow field, and the flames will be diluted-inerted by the resulting water mist some distance away from ignition. This will not only have a very significant effect in the near field of the explosion, but also it may strongly reduce far-field pressures away from the explosion.

In Figure 11 the comparison between experiments and FLACS for pressures inside the rig and into the far field can be seen. By comparing Test 10 and 11 with Test 12 in Figure 9 (all center ignition) and Test 8 and 9 with Test 7 (all end ignition), it can be seen that water deluge brought far field pressures down by about a factor of three. It should be mentioned that in later HSE Phase 3A tests an even better effect was observed. From the plots it can be seen that the effect of water deluge is very well simulated with FLACS, and both near-field and far-field pressures are generally predicted very well. Similar to the previous tests, it can also be seen that limited value is obtained from applying the TNO Multi-Energy curves and that the experiments cannot be captured by one curve. For example, even if the pressure level is adjusted to that observed in the experiments, the TNO predictions of the far-field blast pressures are further reduced.

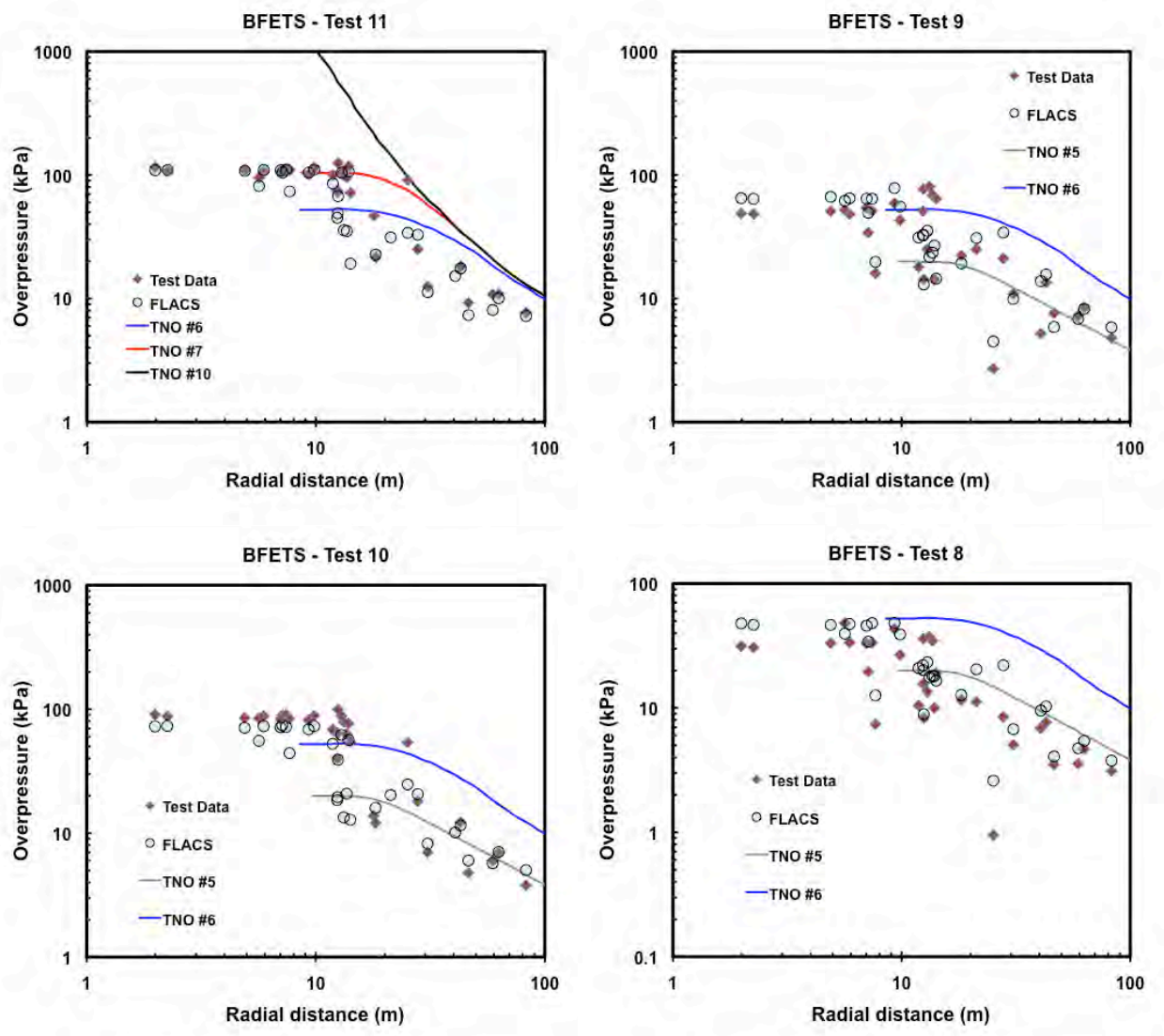

Figure 11: BFETS water deluge simulations compared to experiments, MV57 nozzles 17 liter/m^2/min (upper plots) versus LDN nozzles 27 liter/m^2/min (lower plots), central ignition (left plots) versus end ignition (right plots).

HSE Phase 3A Experiments

After the BFETS experiments in 1998, the UK Health and Safety Executive (HSE) decided to perform a new series of large-scale explosion tests with methane dominated natural gas in cooperation with Advantica. The focus of these experiments was to explore scenarios with less confinement and higher level of congestion. A significant number of tests were performed using water mitigation. There were many interesting observations during the ~45 tests, for instance

- Despite a low degree of confinement very high pressure levels (often > 1000 kPa locally) were observed when the flame traveled 15-25m from the point of ignition to the edge of the geometry/cloud
- In several scenarios, including Test 4 being studied here, deflagration to detonation transition may have taken place as the flame exited from the test geometry. Locally very high pressures were observed at the exits, and from sensor recordings, shock waves could be observed propagating back into the geometry.
- Water deluge had a very good mitigating effect for such low-confinement scenarios, with maximum pressures being reduced from greater than 1000 kPa to 30-50 kPa using as low as 10-15 liter/m^2/min. Water curtains (10m separation) were less effective, as this allowed a significant flame acceleration and pressure build-up between the curtains.
- Test repeatability was investigated, and very significant variations among identical repeated tests were observed. For one of the geometries, a given test was repeated 5 times both with center ignition (alpha-series) and end ignition (beta-series). As expected the highest variability was seen for end ignitions, where some sensors near the ignition showed a factor of two variation among the tests (20-40 kPa), whereas at the far end, pressures varied from 350 to 3500 kPa (factor of ten) at one sensor.

Again in this study we will focus on the far-field blast predictions. We have chosen to simulate the first four experiments in the test series, HSE Phase 3A test 1, 2, 3 and 4. These experiments are all in the same geometry layout, called obstruction level 1 (O1), with solid roof, but no walls. The model of the HSE Phase 3A test geometry is shown in Figure 12. The dimensions are 28m x 12m x 8m; more details about the tests can be found in Table 3.

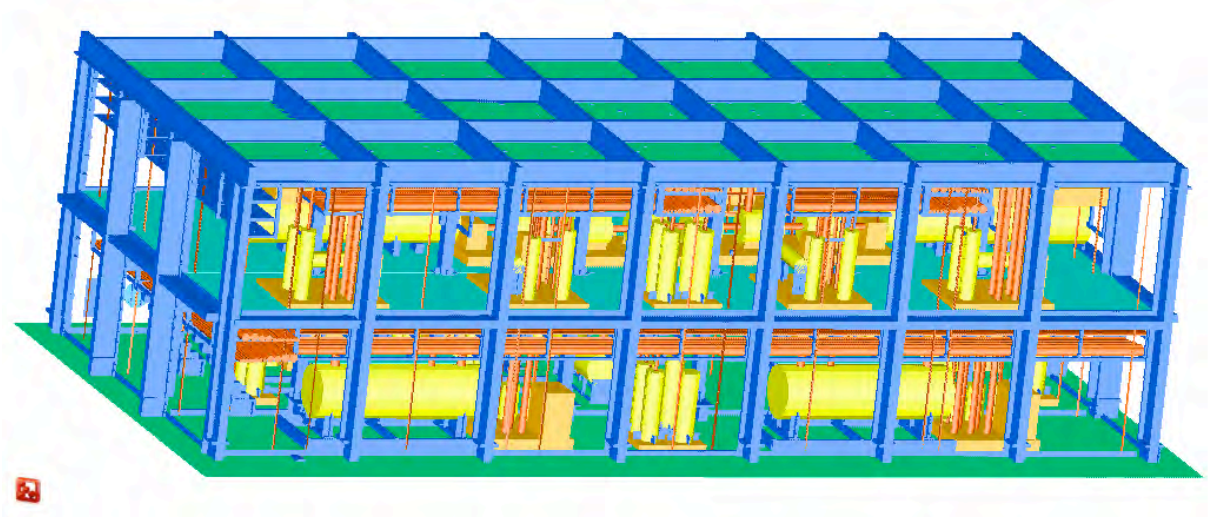

Figure 12: Illustration of the HSE Phase 3A geometry used in this study. The test geometry is similar to the one used for BFETS, but it has been extended in width (8 to 12m), the walls have been removed, and there have been some changes in internal layout.

Table 3: Overview of Advantica HSE Phase 3A tests simulated in this study (Al-Hassan, 1998)

Test	Congestion	Ignition	Confinement	Pressures inside rig
HSE-1	O1	Center Floor	Roof, no walls	50 to 180 kPa
HSE-2	O1	Center Mezzanine	Roof, no walls	40 to 160 kPa
HSE-3	O1	Edge	Roof, no walls	20 to 340 kPa
HSE-4	O1	End	Roof, no walls	15 to > 720 kPa

The selected tests very clearly show how blast pressures for one scenario can significantly differ from another scenario, where the only parameter varied is the ignition location. In Figure 13 the simulated maximum pressure distribution for Test 4 is shown. The test geometry, in which the gas cloud was ignited, is illustrated with a rectangular box in Figure 13. It can be seen that very low pressure levels are found around and behind the ignition location, whereas the highest pressures can be found near the opposite end and just outside the geometry. The very non-symmetrical pattern is typical for many situations with asymmetric ignition sources. Using a traditional blast approach (*e.g.*, TNO Multi-Energy) considering pressure waves from the center of the gas cloud will tend to under-predict the pressures outside the geometry, as directional/dynamic effects like this are not considered.

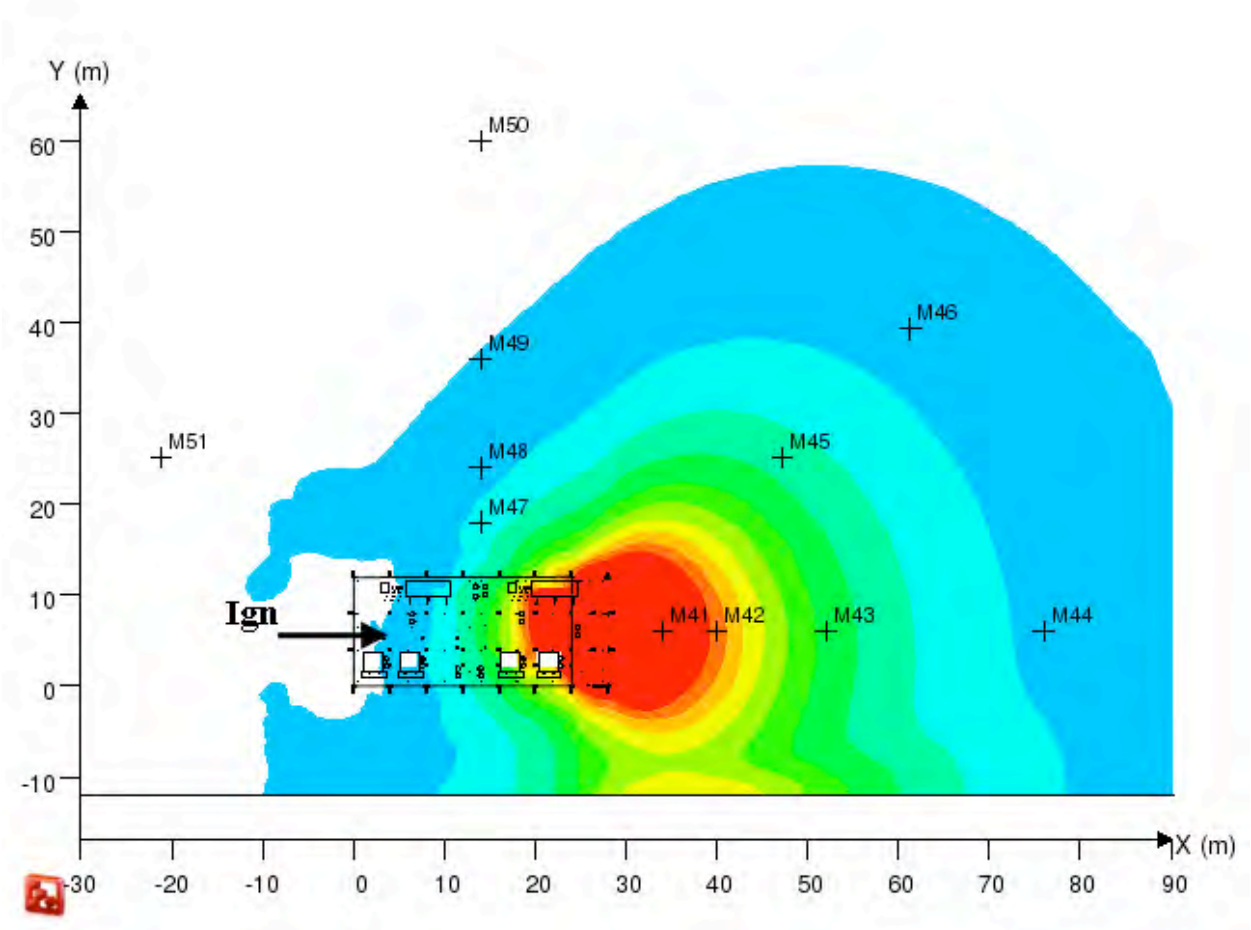

Figure 13: Example of non-symmetric blast pattern from simulation of HSE Phase 3A Test 4. External sensor locations are shown on the plot.

The HSE Phase 3A tests were simulated using both a 1m grid and a 0.67m grid. The grid sensitivity was limited, and the finer grid was reported here.

Comparisons of simulated and experimental overpressures for sensors inside the geometry (source pressures) and external sensors (far-field pressures) are shown in Figure 14. External sensor locations shown in Figure 13 were used in the present study. For these tests all experimental pressures have been smoothed and reported using a 1.5ms running average in order to remove noise or other-anomalies. From the plots we can see that there are large directional effects in the far-field pressures (in particular for test 3 and 4), where far-field overpressures larger than those predicted by the strong TNO Multi-Energy curve were observed. FLACS simulations appear to accurately predict all trends and directional effects, however show some under-prediction for certain conditions. This is particularly true for Test 4 where the explosion strength was also under-predicted. The overpressure recordings before smoothing in test 4 were as high as 1700 kPa, and upon closer evaluation of the pressure curves, indicate that a transition to detonation (DDT) may have taken place when the flame exited the test geometry. While there are ongoing efforts to model DDTs in FLACS (namely for hydrogen explosions, Middha and Hansen, 2008), the potentially observed DDT in the present experiment cannot be properly captured by FLACS and may be a contributing factor to the observed under-prediction of blast waves in Test 4. Other explanations may involve the method of recording experimental pressures. Two of the tests, Test 3 and Test 4, have a very non-symmetrical development of the flame. All the far-field blast sensors (skimmer-plates) were placed with an assumption on where the pressure waves will arrive. Unfortunately, it is very likely that many of the sensors received the main blast waves from directions different than originally anticipated, and some sensors may also have received contributions and reflections from multiple directions during the experiment. It should thus be expected that many of the recordings are higher than the theoretical side-on pressure. Finally, a third reason for under-predicting the experiments, especially in the far field, is that the CFD-simulations will not manage to reproduce the very sharp leading edge of the shock wave, and due to smearing of the front, slightly under-estimate the maximum pressure value.

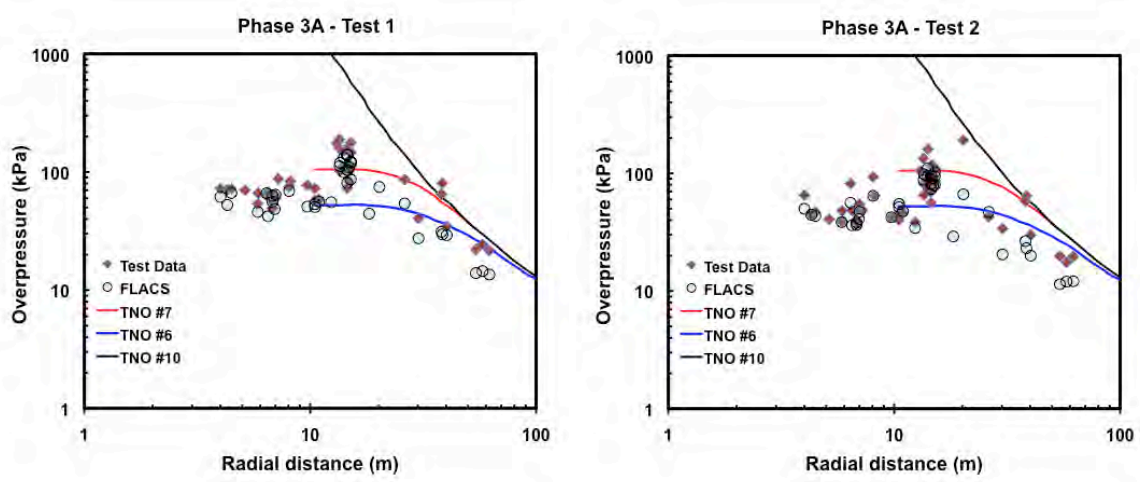

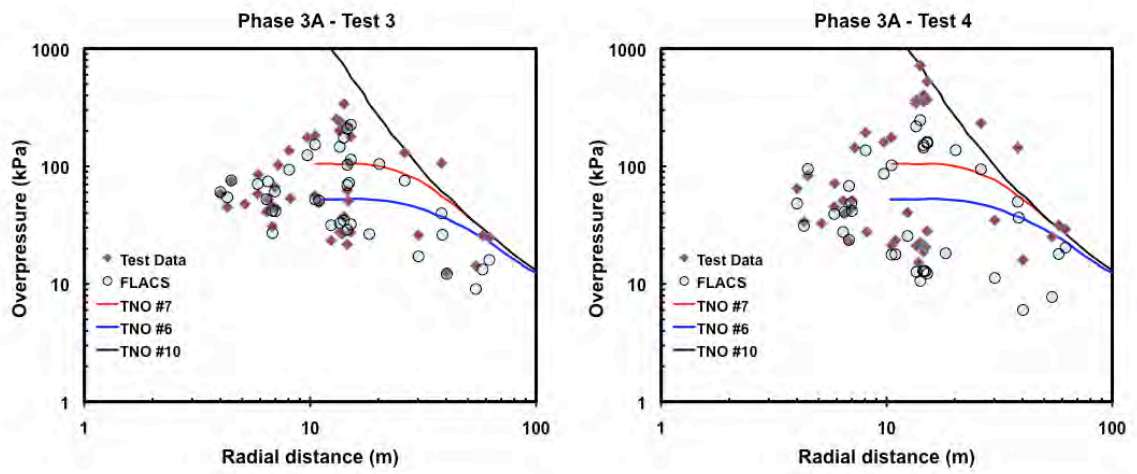

Figure 14: HSE 3A simulations compared to experiments, center ignition (upper left), center floor (upper right), edge ignition (lower left) and end ignition (lower right).

Phase 3B Experiments

Phase 3B was a multi-sponsor JIP supported by ten oil and gas companies. The project was carried out by Advantica, GexCon and Shell Global Solutions. Experiments were performed both at GexCon (medium scale) and Advantica (large scale) test sites. Among the main ambitions of the project were to study ignited dispersion experiments, and to learn more about the explosion development in realistic gas clouds that is distinct from explosions of premixed stoichiometric clouds. GexCon performed about 100 such tests in the medium-scale geometry ($50m^3$), whereas Advantica performed 20 large-scale experiments (28x12x8m rig, approximately $2600m^3$) in which a gas cloud formed from a gas release was ignited. The findings from these experiments were numerous. Regarding the level of overpressure, it was found that for the selection of tests performed in this project most experiments would give much lower pressures than obtained with a full stoichiometric cloud. However, in some cases the overpressure level from ignited releases approached those seen for full premixed stoichiometric clouds, and at the medium-scale, even higher-pressure levels were observed in certain tests (flame acceleration was initially enhanced by jet induced turbulence).

One further ambition of the Phase 3B project was to generate validation data for the probabilistic risk assessment approach proposed in Norsok (2001), in which stoichiometric gas clouds of various sizes are ignited with probabilities determined by an extensive dispersion and ventilation study using computational fluid dynamics (*e.g.*, FLACS). Advantica performed six experiments where premixed near stoichiometric cloud sizes ranging from 10% to 100% of the test rig volume were exploded. The model of the Phase 3B test geometry used for these tests is shown in Figure 15, where the lower image is a 2D plot showing the positions of the external pressure measurements (sensors 26 to 30). We used these experiments in the present study to illustrate pressure wave generation from partially filled compartments.

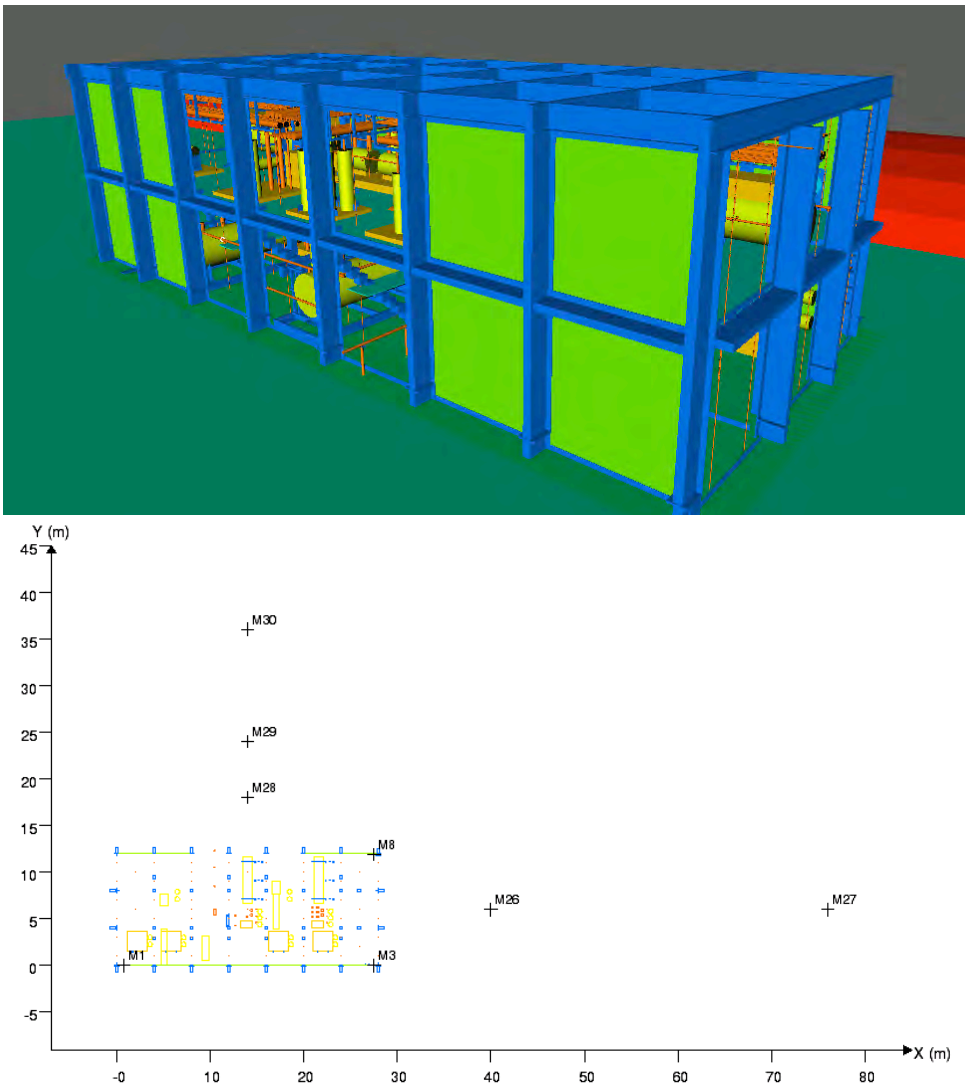

Figure 15: Illustration of Phase 3B geometry and pressure sensor locations

Characteristics for the different scenarios (gas cloud location/size/shape) can be found in Figure 16 and Table 4. The same ignition location was used in all tests (X=16m, Y=4.5m and Z=4.3m).

Table 4: Overview of Phase 3B Partial Fill Explosion Experiments simulated

Test	**Cloud Size**	**Ignition**	**Confinement**	**Pressures inside rig**
PF TEST 1	19% (8x8x8m)	Center	Solid Roof	4-10 kPa
PF TEST 2	10% (4x8x8m)	Edge	Open wall areas	2-5 kPa
PF TEST 3	43% (12x12x8m)	Center	E, W, N	15 to 60 kPa
PF TEST 4	43% (12x12x8m)	Edge	Each 12m x 8m	10 to 40 kPa
PF TEST 5	100% (28x12x8m)	Center		45 to 240 kPa
PF TEST 6	19% (8x8x8m)	Edge		3 to 13 kPa

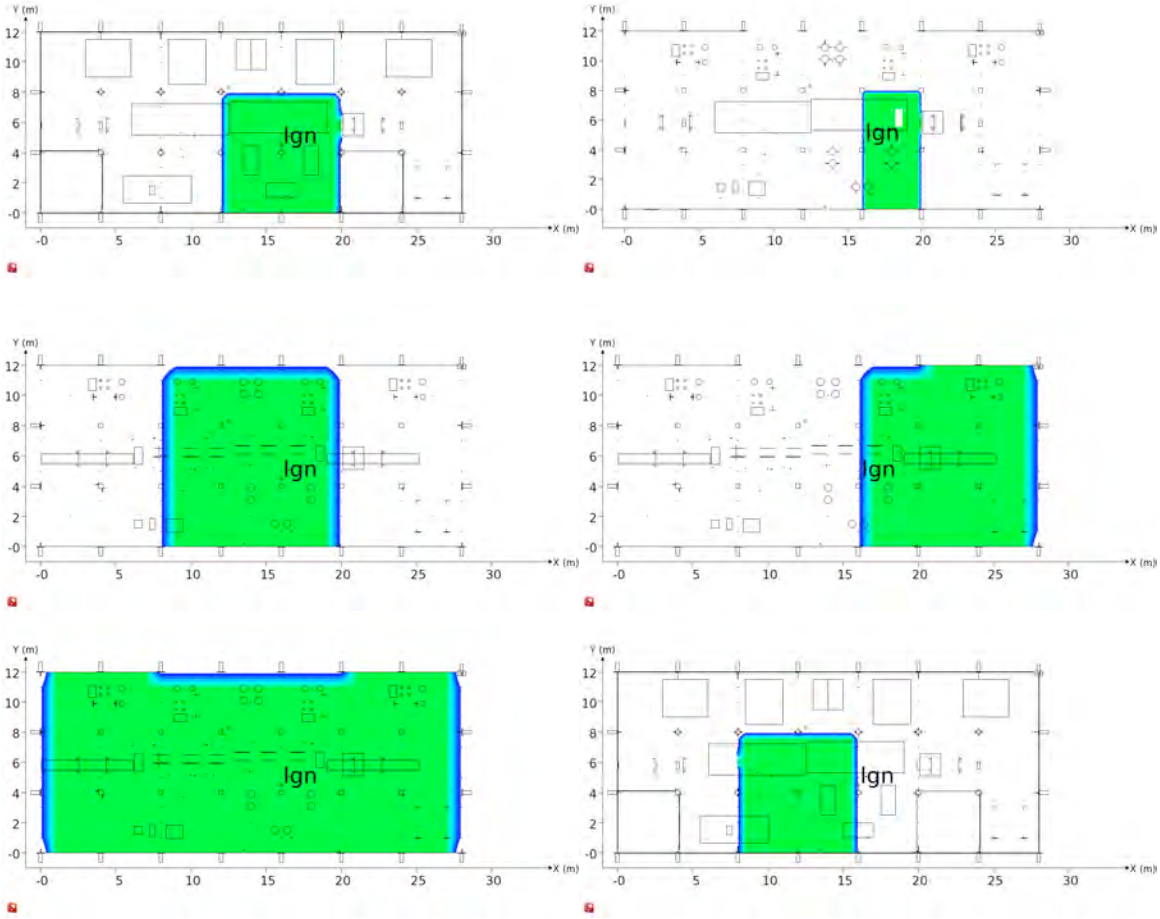

Figure 16: Phase 3B experiments, 6 different cloud sizes and locations are illustrated.

In Figure 17 the predictions from the simulated pressures are compared to the experimental values. It can be seen that trends regarding pressure decay with distance are well reproduced, but that some of the experimental results are over-predicted (*e.g.*, tests 1, 4 and 6). There may be many reasons for the pressure over-predictions for certain tests. For example, end ignitions present a significant challenge due to the difficulty in obtaining homogenous concentrations throughout the entire gas cloud. For these cases, it is worthwhile to note that the gas concentration may be slightly lower near the edge of the gas cloud in the region near ignition, and this may strongly affect the initial flame acceleration and the resulting overpressures.

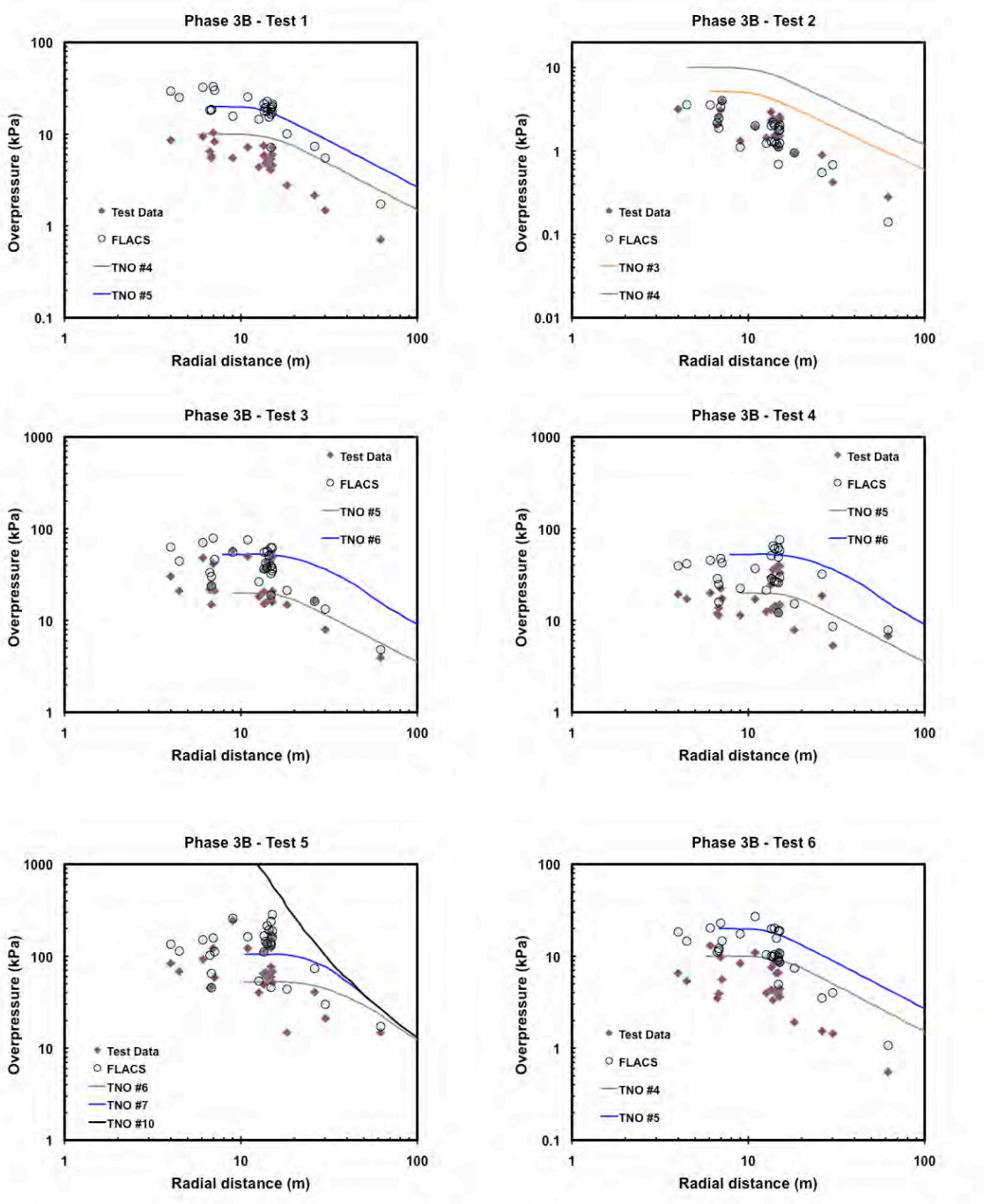

Figure 17: Phase 3B simulations versus experiment (For detailed scenario description for each test see Figure 16.).

NIOSH LLEM Experiments

The last test series we will use for our evaluation are some experiments performed inside tunnels of Lake Lynn Experimental Mines (Zipf *et al.*, 2007). The purpose of including these

experiments is to illustrate how pressure wave decay will become significantly different when confined inside a tunnel system. Two different experimental configurations were simulated, and consist of a single drift tunnel and a three-drift tunnel. The model of the Lake Lynn Experimental Mines tunnels are shown in Figure 18, the one-drift tunnel is referred to as the D-drift, whereas the three-drift tunnel is referred to as the B-drift tests. GexCon blind simulated a total of six experiments in these two test configurations as part of a commissioned study for NIOSH in 2006 with the following performance:

Table 5: FLACS blind prediction performance reported by (Zipf *et al.*, 2007) for two different sensors in each experiment

Test	Cloud Size	Geometry	Ignition	Test (kPa)		FLACS (kPa)	Deviation
468	3.66x6x 2m	D-drift	Inner	#1	21.5	18.7	-13%
			end	#10	18.6	17.6	-5%
469	8.23x6x2m	D-drift	Inner	#1	58.9	57.5	-3%
			end	#10	48.1	51.9	+8%
470	12.2x6x2m	D-drift	Inner	#1	75.0	76.3	+2%
			end	#10	74.8	71.0	-5%
484	12.2x6x2m	B-drift	Inner	#10	83.9	71.2	-15%
			end	#526	29.4	28.9	-3%
485	18.3x6x2m	B-drift	Inner	#10	101.3	97.6	-4%
			end	#526	34.1	42.3	+24%
486	18.3x6x2m	B-drift	Center	#10	48.1	57.1	+19%
				#526	24.9	23.1	-7%

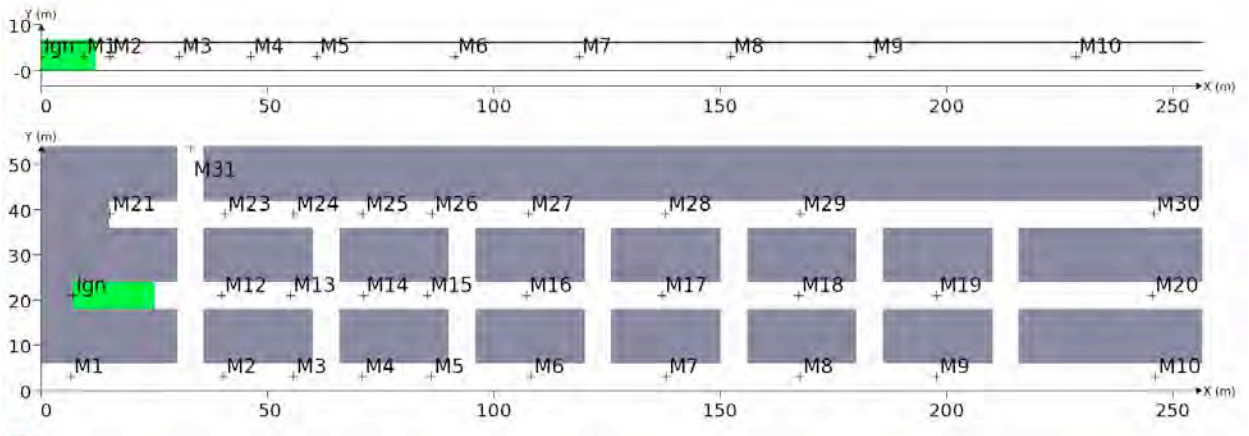

Figure 18: Illustration of LLEM geometry model with pressure sensors, the D-drift tunnel is shown in the upper plot and the B-drift tunnel in the lower plot. The numbering of sensors may deviate from that used in the experiments.

To illustrate the pressure decay in tunnels, and FLACS' ability to model this phenomenon, we have selected two of the experiments listed above. These are the strongest explosion tests in each scenario, test 470 in the D-drift and test 485 in the B-drift. In Figure 19, the pressure development in the FLACS simulation as the pressures are propagating down the tunnels is

compared to the observations. It can be seen that the simulated pressure decay follows the experimental observations closely. The TNO Multi-Energy model is illustrated in the plots, and is clearly not very useful here due to the high degree of confinement. This should be no surprise as it never was the intention of the TNO Multi-Energy model to handle tunnel scenarios. In Figure 20 three pressure curves are selected for each of the two tests and compared to simulated pressures. The first point is chosen in the inner end of each drift, where the highest explosion pressures were seen, the third point around 230m from the ignition, and the point in the middle was around 130-150m from ignition. By studying these curves in detail, it is evident that the physics reproduced in the FLACS-CFD software closely resembles the observed physics from the experiments. One interesting observation is that the losses for the pressure wave propagation in the single tunnel are much less than those observed in the more complex three-drift tunnel.

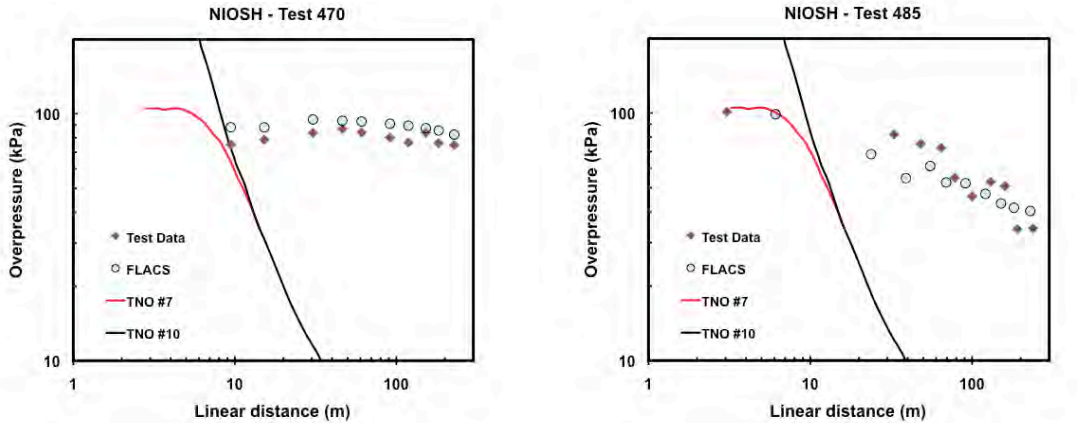

Figure 19: Example of pressure decay with distance, test 470 (upper, one drift tunnel with 150m^3 gas cloud) and test 485 (lower, 3-drift tunnel with 220m^3 gas cloud)

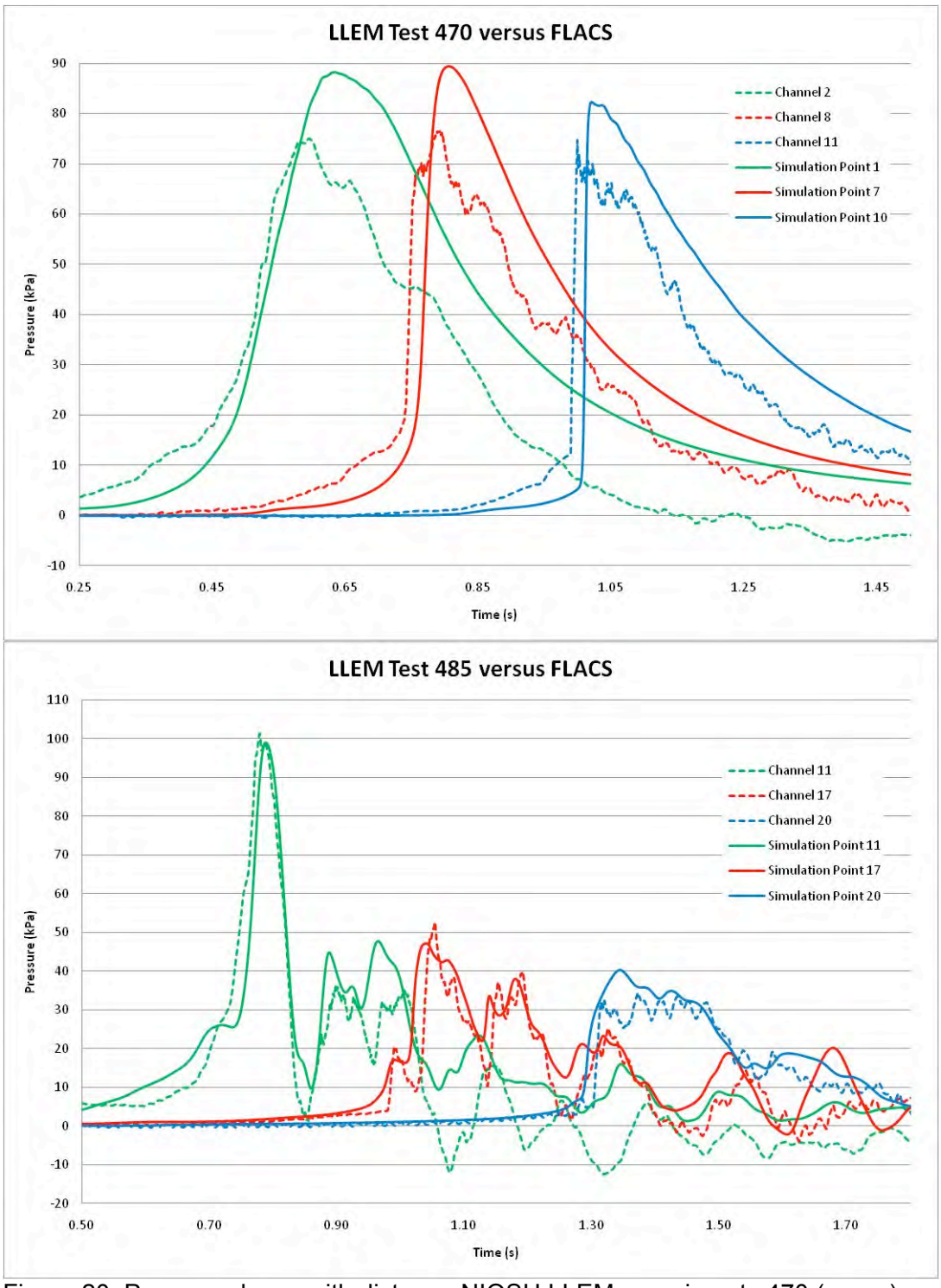

Figure 20: Pressure decay with distance NIOSH LLEM experiments 470 (upper) and 485 (lower) versus FLACS

Conclusion Validation Study

In general, FLACS simulations were reasonably close to experimental data for source explosion pressures for the extensive and vastly different experimental configurations. These included the various perturbations of unconfined symmetric experiments, partially confined asymmetric experiments, and completely confined tunnel experiments. FLACS predictions for the far-field pressures were reasonable for the weaker explosions, but FLACS generally under-predicted the far-field pressures for strong explosions. Details of these conclusions are discussed next. Finally, ongoing work involving a proposed methodology evaluating far-field pressures is discussed.

The six MERGE experiments were unconfined, symmetric cases and were conducted at both medium and large scales. For the six MERGE experiments, FLACS predicts the explosion source pressures well for the six cases as well as the far-field pressures for weaker explosions (Merge C and E). However, FLACS under predicts the far-field pressures by approximately a factor of two for the strong explosion cases (MERGE A, B, D, C*). These results were generally independent of the grid resolution. The discrepancy in the far-field predictions for the strong explosion cases is likely due to: (1) numerical smearing of the abrupt pressure rise (discontinuity in the shock wave) observed in experiments and (2) potential contribution of wave reflections in the far-field sensors that result in very thin (trivial impulse) pressure spikes. Methods for improving predictions will be discussed at the end of this section.

The BFETS experiments were conducted in a large scale, asymmetric, offshore module. Experiments evaluated end and central ignition cases for both low-obstacle density and high-obstacle density test geometries. FLACS predictions were generally good for both near-field source pressures and external far-field pressures. FLACS accurately predicted the details of the asymmetric source pressures within the module for both weak and strong explosions. Predictions were slightly under-predicted in the far field for the strong explosions and were very close for weak explosions. Experiments were also conducted employing water deluge systems. These experiments, which were predicted reasonably well by FLACS, confirmed the benefit of water deluge in limiting far-field pressures.

The HSE Phase 3A experiments were conducted in a large scale, asymmetric, offshore module. Experiments evaluated end and central ignition cases in a high-obstacle density test geometry. The Phase 3A experiments involved completely filling the module, while the Phase 3B experiments performed in an equally sized, but somewhat modified geometry, were partial fills. FLACS predicted the source pressures reasonably well for most Phase 3A tests, which included strong non-symmetric pressures in the near field (*i.e.*, pressures differing by more than an order of magnitude at similar distances from the center of the module). Similar to the MERGE experiments, FLACS generally under-predicts the far-field pressures. There was more scatter observed in the predictions and the Phase 3B results, where FLACS over-predicted some of the experimental pressures.

The NIOSH tests were conducted in enclosed tunnels. The first geometry consisted of one straight tunnel, while the second geometry included three parallel tunnels interconnected by multiple perpendicular tunnels. FLACS accurately predicted the magnitude and behavior of the

explosion pressures observed in the experiments, namely the faster pressure decay was predicted for the three parallel tunnel case as compare to the single tunnel. In addition, the pressure maximum and shape of the pressure trace (impulse and time duration) were accurately captured in the simulations.

For all of the experiments, the equivalent TNO Multi-Energy curves were also plotted against the experimental data. For the unconfined, symmetric MERGE experiments, the TNO Multi-Energy method generally over-predicted the experimental data and provided an upper bound for the overpressures. Some empirical energy scaling has been suggested (van der Berg and Mos, 2005) to improve predictions, but requires knowing the source pressure beforehand. For the partially confined asymmetric cases, a single TNO Multi-Energy curve could not accurately capture the distribution in source explosion pressures, but again would typically predict an upper bound for the observed overpressures. For some sensor locations, significant over-predictions of the far-field pressures were observed due to geometry effects (greater than a factor of five). While the TNO Multi-Energy curves generally provided an upper bound for symmetric and asymmetric experiments, some experimental pressures were higher than the TNO Multi-Energy curves in the partially confined, asymmetric cases due to strong directional effects. Such effects should be considered, especially if the goal is to estimate the fuel involved in an accidental explosion. Finally, for completely enclosed tunnel explosions, the TNO Multi-Energy method was not designed for such geometries and cannot accurately be applied.

For the strong explosion cases, FLACS generally (with the exception of BFETS) under-predicts the far-field overpressures. As previously discussed, the far-field overpressure is the "side-on" or pressure (P_s) that arrives parallel to the sensor. Theoretically, the side-on pressure is independent of any pressure wave reflections due to contributions normal or "head on" to the sensor, which can result in significantly higher recorded pressures and possible spikes. While experiments were designed to avoid such contributions, it is difficult to know *a priori* from what direction pressure waves may be generated. In addition, other short duration (negligible impulse) pressure spikes have been observed in some sensor readings, and while they may be associated with wave reflections in the sensor, the exact cause of such anomalies is not known for some of the experiments. Therefore the more recent experiments at Advantica test site (BFETS, HSE 3A and Phase 3B) have incorporated averaging techniques in an attempt to filter out anomalous or unwanted pressure spikes in the far-field data.

In addition, for strong explosions (*i.e.*, TNO Multi-Energy curves $\geq$ 6), it has been previously demonstrated that the blast wave begins to shock-up as it propagates from the source. This results in a shock wave or a nearly discontinuous pressure trace, with a sudden and abrupt increase in pressure, followed by an exponential decay of the pressure. In order to numerically resolve this front, at least 4-5 grids are required in CFD calculations, which becomes numerically prohibitive if one were to resolve the entire explosion on that scale. As such, FLACS simulations will numerically "smear" this sharp pressure front. Oftentimes the shape of the positive phase of the far field pressure wave is estimated as a triangular pulse, with an instantaneous increase in pressure to P_s, followed by a linear decay to ambient pressure. Current work at GexCon is evaluating the postprocessing of the pressure-time curves in order to more accurately predict the magnitude of the overpressure and the shape of the impulse. One such method involves linearly extrapolating the decay tail of the pressure profile to a vertical plane.

This vertical plane is determined by maintaining the impulse, or integrated pressure profile, and is shown in Figure 21. Where the two lines intersect is the "corrected" prediction of far-field pressure. Figure 21 shows the example method compared against the experimental pressure profile for sensor 13 in the Merge C* experiment.

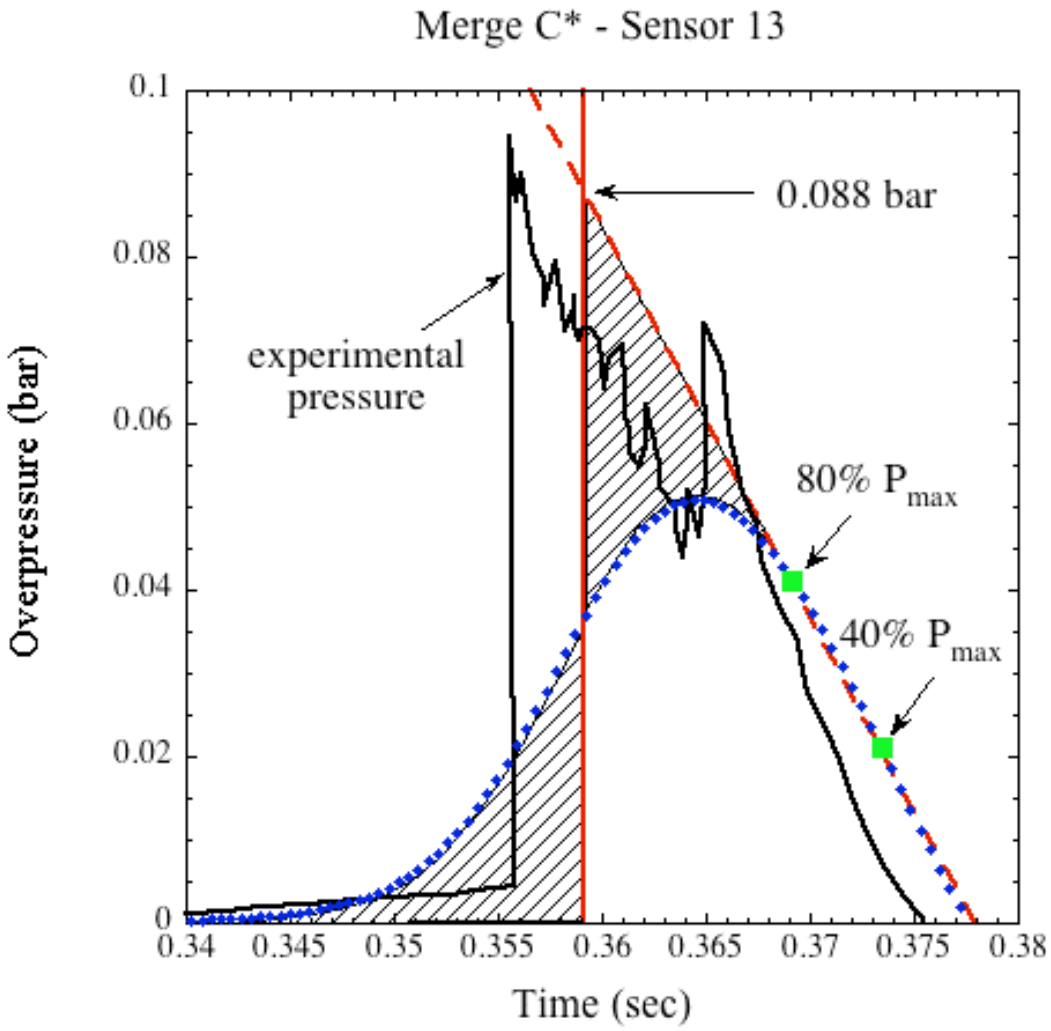

Figure 21: Proposed method for post-processing FLACS far-field pressures (strong explosions)

Proposed Method for Blast Screening Calculations of Facilities

In the introduction we discussed challenges associated with blast siting studies when CFD is used on real installations. Oftentimes a CAD model that can be utilized in the explosion

consequence study does not contain adequate detail or simply does not exist. As such, it may require numerous man-months of modeling work to create a decent geometry representation. Since geometry detail level, as well as confining walls and decks, may be very important for the generation of explosion overpressures and blast waves, such information will be required to achieve accurate predictions.

In the following, we propose a screening approach for CFD tools, in which the main confining structures which may influence the development of the explosion are implemented manually (walls, decks, and a few larger objects), whereas a simplified array of beams are used to represent the finer geometry details. One challenge with such an approach is how to define the representative congestion level, *i.e.* obstruction density. A similar methodology, where only the finer geometry details are anticipated, anticipated congestion method (ACM), is frequently used in offshore platforms during the early design stages when the details of the modules are not complete. Since the assumptions in the proposed approach are even coarser, it will in the following be referred to as Representative Congestion Model.

When considering the physics of explosions, it is evident that the turbulent wakes behind the objects in the flame path play an important role in how the explosion develops. One natural assumption when looking for parameters important for flame acceleration will therefore be to consider the object surface area in each direction to be a main parameter. It is therefore possible to define a surface area of the objects (A) and compare that with the available volume (V), resulting in an average representative congestion level or an A/V ratio (dimension m^2/m^3). This idea can readily be observed in the MERGE experiments. For example, in the medium scales experiments the highest source pressures (170 kPa) were observed with A/V = 21.7, the mid-range source pressures (70 & 77 kPa) were observed with A/V = 10 & 12, and the lowest source pressure (10.8 kPa) with A/V = 5. Similar trends were observed at the large scale, where higher source pressures (90 kPa) were observed with A/V = 5 and lower source pressures (14.2 kPa) were observed with A/V =2.5. Notice that the scale of the experiment is a very important parameter, and the A/V ratios for different scales should not be compared. If a geometry is linearly scaled by a given factor, the A/V is reduced by the same factor.

Methodology

While this is currently still under investigation the main goal was to provide a method that provides reasonably accurate results of overpressures while spending considerably less time developing complex geometries. Using an array of box objects to account for interior anticipated congestion was considered.

To obtain the surface area of realistic geometries (*i.e.*, BFETS and HSE Phase 3B), a script was used to calculate the surface area of all sides of each object in the structure. These were then added to give a total combined area. Larger surfaces associated with walls and decks, which would be manually defined, were removed from the calculation and the remaining areas were used to construct an anticipated congestion model. A model geometry was next constructed with the same interior congestion surface area as the actual model. The simplified congestion consisted of box elements that were 0.25m by 0.25m (25-50% of grid cell size) and would span the length of the structure. These box elements were then evenly spaced in the three orthogonal directions to form an array. The 0.25 width of the beam was chosen to be a subgrid scale (25%-

50% of the grid cell size in each direction). The frequency of the congestion was then adjusted until the same total interior surface area was achieved. Examples of anticipated congestion models for HSE Phase 3B can be seen in Figure 22 and for BFETS in Figure 23.

The modified geometry was then tested using the same criteria of gas could size, location etc., and evaluated to compare the resulting overpressures.

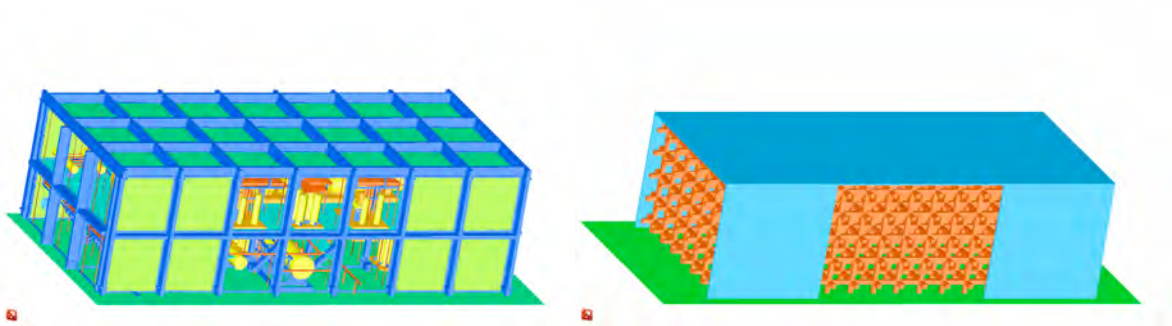

Figure 22: Phase 3B actual geometry model (left) and representative congestion model (right)

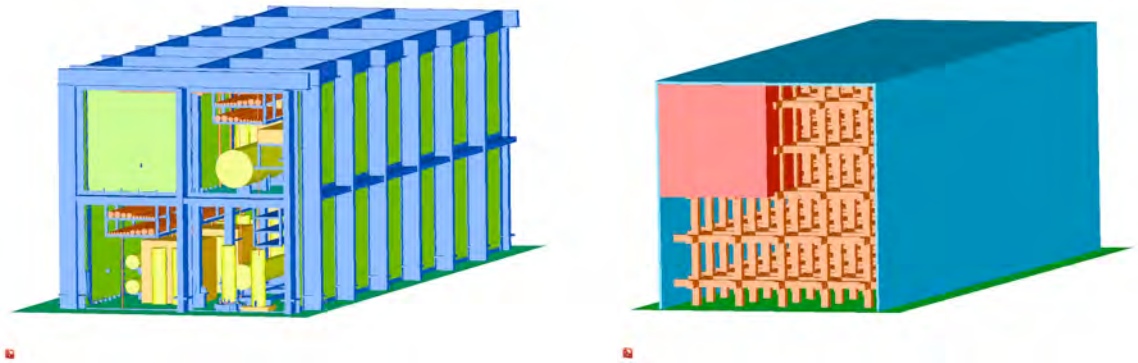

Figure 23: BFETS actual geometry model (left) and representative congestion model (right)

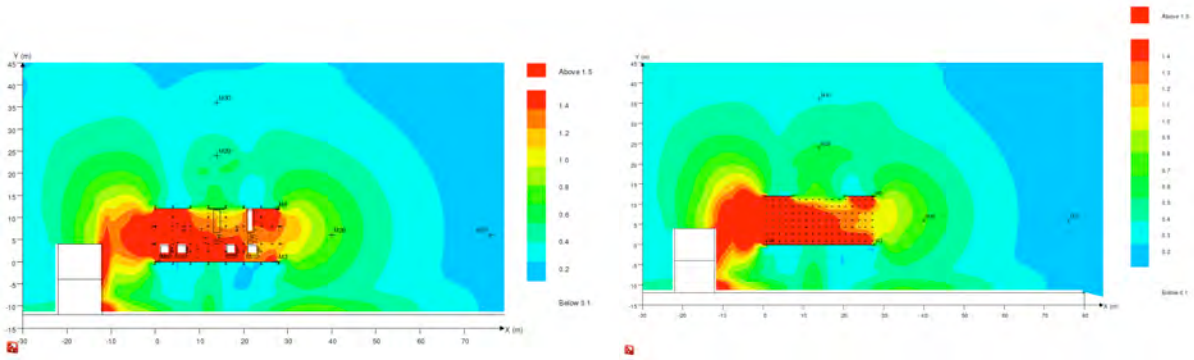

Figure 24: Maximum predicted overpressures for Phase 3B Test 5 (100% gas cloud): actual geometry (left), representative congestion model (right)

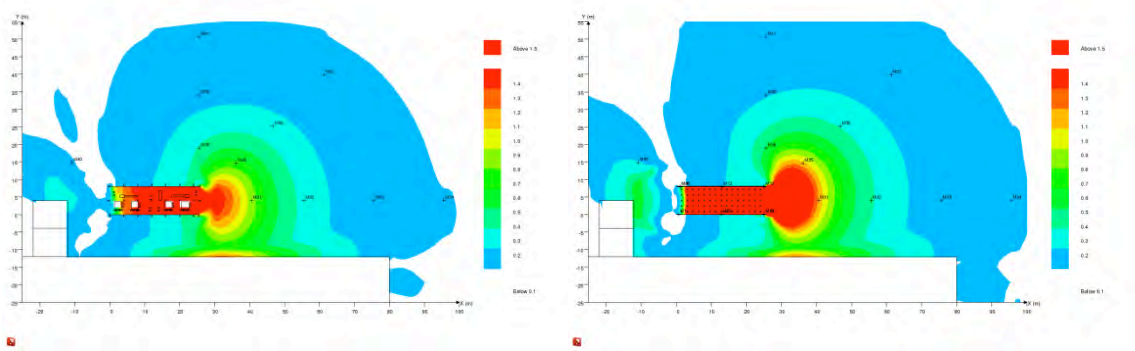

Figure 25: Maximum predicted overpressures for BFETS test 7 (end ignition): actual geometry (left), representative congestion (right)

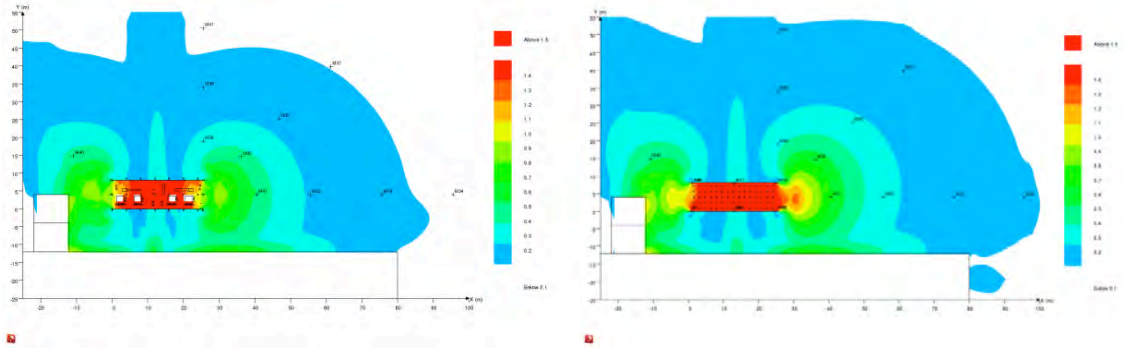

Figure 26: Maximum predicted overpressures for BFETS test 12 (center ignition): actual geometry (left), representative congestion (right)

From Figure 24, 25 and 26 it can be seen that the simulated blast loads with the representative congestion approach are comparable or slightly higher than found with the real geometry. The probable reason for the slightly higher results is that representative congestion elements are more evenly distributed (the effect of congestion elements on explosion pressures can be reduced if they are too closely spaced).

Conclusions Representative Congestion Method

A simplified approach to the CFD modeling of blast waves for siting studies in and around onshore plants has been proposed and evaluated. The approach, using an obstacle area to volume (A/V) scaling, is supported by observations of explosion pressures in the MERGE geometries. When simulating known explosion experiments using the A/V method, this approach produced very similar or slightly more conservative estimates compared to applying actual test geometries. It is thus concluded that the approach seems promising.

If the approach shall be applied on a real onshore plant, it may not be trivial to determine the exact A/V ratio. The recommended approach will then be to analyze comparable geometries from other studies performed in similar plants, and based on prior studies, estimate a representative A/V ratio. Thereafter the main decks, walls, tanks and larger objects will be modeled before filling in the representative congestion level in the rest of the congested areas of the plant.

Assuming that the initial screening study will be representative or slightly conservative, the user will always have the possibility to replace the simplified modeling with a better geometry model if a more accurate study is to be performed.

Acknowledgments

GexCon would like to acknowledge the NIOSH sponsored mine explosion project NIOSH IC 9500.

References

Al-Hassan, T. Johnson, D.M. "Gas explosions in large scale offshore module geometries: Overpressures, mitigation and repeatability, presented at OMAE-98, Lisbon, Portugal, 1998

Baker, W.E., Cox, P.A., Westine, P.S., Kulesz, J.J. and Strehlow, R.A. Explosion Hazards and Eualuation, Fundamental Studies in Engineering, 5. Elsevier Scientific Publishing Company, Amsterdam, (1983)

Bakke, J.R. and Hansen O.R., 2003, Probabilistic analysis of gas explosion loads, FABIG Newsletter , Issue No. 34, January 2003

Buncefield investigation report (progress report)
http://www.buncefieldinvestigation.gov.uk/report.pdf

CSB, 2007, Refinery Explosion and Fire, BP Texas City, US Chemical Safety and Hazard Investigation Board Report no 2005-04-I-TX

CSB Investigation Report 2007-03-I-MA, May 2008

Hanna, S.R., Hansen, O.R., Ichard, M. and Strimaitis, D., 2009, CFD model simulation of dispersion from chlorine railcar releases in industrial and urban areas, Atmospheric Environment 43 (2009), 262–270

Hansen, O. R., Melheim, J. A., Storvik, I. E. CFD-Modeling of LNG dispersion experiments. In: AIChE Spring National Meeting, 7th Topical Conference on natural gas utilization. Houston, USA, April 23–26, 2007.

Hjertager, B.H., 1985. Computer simulation of turbulent reactive gas dynamics. J. Model. Identification Control 5, 211–236.

Hoorelbeke, P., Izatt, C., Bakke , J.R., Renoult, J., and Brewerton, R.W., 2006, Vapor Cloud Explosion Analysis of Onshore Petrochemical Facilities: ASSE-MEC-0306-38

Ichard, M. Hansen O. and Melheim, J. 2009, MODELLING OF FLASHING RELEASES AROUND BUILDINGS, presented AMS meeting Phoenics, Paper J-14, January 2009

Johnson, D.M. *et al.* "Investigation of Gas Dispersion and Explosions in Offshore Modules", OTC-paper 14134, Houston 6-9 May 2002

W.P.M. Mercx *et al.* (1994), Modelling and experimental research into gas explosions, Overall Report of the MERGE Project, CEC contract: STEP-CT-0111 (SSMA)

Mercx, W.P.M., 1996, Extended Modelling and Experimental Research into Gas Explosions, Final Summary Report, CEC EMERGE Project Report, EV5VCT930274 (TNO)

Middha, P., & Hansen, O. R. (2008). Estimating the consequences of Deflagration to Detonation Transition (DDT) in hydrogen explosions. Process Safety Progress, 27(3), 192–204.

Middha, P, and Hansen, O.R. 2009, CFD simulation study to investigate the risk from hydrogen vehicles in tunnels, International journal of hydrogen energy 34 (2009) 5875–5886

NORSOK Z-013, 2001. Risk and emergency preparedness analysis, Norsok standard. Available from Standard Norge, Postboks 242, N-1326 Lysaker, Norway.

Pierorazio, A.J., Thomas, J.K., Baker, Q.A and Ketchum, D.E 2005, An update to the Baker-Strehlow-Tang vapor cloud explosion prediction methodology flame speed table, Process Safety Progress, Volume 24, Issue 1, pages 59-65.

Puttock, J.S., 1995, Fuel Gas Explosion Guidelines, the Congestion Assessment Method, 2nd European Conference on Major Hazards On- and Offshore, Manchester, UK, 24-26 September 1995.

SCI, 1996, Joint Industry Project on Blast & Fire for Topside Structures, Phase II, Interim Information Release.

Selby, C., Burgan, B. "Blast and fire engineering for topside structures, Phase 2, Final summary report", Steel Construction Institute, UK, Publication number 253, 1998.

van den Berg, A.C., 1985, "The Multi-Energy Method: A Framework for Vapour Cloud Explosion Blast Predictioin," Journal of Hazardous Materials, Vol. 12, pp. 1-10.

van den Berg, A.C. and Mos, A.L., 2005, "Research to improve guidance on separation distance for the multi-energy method (RIGOS)", Health & Safety Executive Research Report 369.

van Wingerden, K., Hansen, O.R. and Foisselon, P. 1999, Predicting Blast Overpressures Caused by Vapor Cloud Explosions in the Vicinity of Control Rooms, Process Safety Progress Vol 18, No 1, pp 17-24

van Wingerden, C.J.M., Hansen O.R. and Teigland, R. 1995, Prediction of the strength of blast waves in the surroundings of vented offshore modules, 4th international conference of Offshore Structures-Hazards, Safety and Engineering Working in the New Era, London, England, 12-13 December 1995.

Zipf, R.K., Sapko, M.J., and Brune, J.F., 2007, "Explosion Pressure Design Criteria for New Seals in U.S. Coal Mines", U.S. Department of Health and Human Services, Public Health Service, Centers for Disease Control and Prevention, National Institute for Occupational Safety and Health, DHHS (NIOSH) Publication No. 2007-144, Information Circular 9500, 2007 July; :1-76.